Author's preprint copy for article published in *Organic Geochemistry*
(https://doi.org/10.1016/j.orggeochem.2020.104080)

Effects of temperature and pH on archaeal membrane lipid distributions in freshwater wetlands

J. Blewett[1,2]*, B.D.A. Naafs[1,2]*, A.V. Gallego-Sala[3], R.D. Pancost[1,2], the 'T-GRES peat database collaborators'

[1]Organic Geochemistry Unit, School of Chemistry, and School of Earth Sciences, University of Bristol, Bristol, UK

[2]Cabot Institute for the Environment, University of Bristol, Bristol, UK

[3]School of Geography, University of Exeter, EX4 4RJ, UK

*Corresponding authors: jerome.blewett@bristol.ac.uk and david.naafs@bristol.ac.uk

Abstract

Freshwater wetlands harbour diverse archaeal communities and associated membrane lipid assemblages, but the effect of environmental factors (e.g. pH and temperature) on the distribution of these lipids is relatively poorly constrained. Here we explore the effects of temperature and pH on archaeal core-lipid and intact polar lipid (IPL) derived core lipid distributions in a range of wetlands. We focus not only on the commonly studied isoprenoidal glycerol dialkyl glycerol tetraethers (isoGDGTs), but also widen our analyses to include more recently identified but relatively widespread archaeal lipids such as isoGDGT isomers, methylated isoGDGTs (Me-GDGTs), and butanetriol and pentanetriol tetraethers (BDGTs and PDGTs). Based on multivariate analysis and a globally distributed set of wetlands, we find that the degree of isoGDGT cyclisation does increase along with

temperature and pH in wetlands; however and unlike in some other settings, this relationship is obscured in simple scatterplots due to the incorporation of isoGDGTs from highly diverse archaeal sources with multiple ring-temperature or ring-pH relationships. We further show that the relative abundance of early eluting to later eluting isoGDGT isomers increases with pH, representing a previously unknown and seemingly widespread archaeal membrane homeostasis mechanism or taxonomic signal. The distribution and abundance of crenarchaeol, a marker for Thaumarchaeota, demonstrates that in wetlands these Archaea, likely involved in ammonia oxidation, are restricted primarily to the generally dryer, soil/sediment surface and typically are more abundant in circumneutral pH settings. We identify Me-GDGTs and Me-isoGMGTs (homologs of isoGDGTs and isoGMGTs, but with additional methylation on the biphytanyl chain) as being ubiquitous in wetlands, but variation in their abundance and distribution suggests changing source communities and/or membrane adaptation. The high relative abundance of BDGTs and PDGTs in the perennially anoxic part of the peat profile (catotelm) as well as their elevated abundance in a circumneutral pH wetland is consistent with an important input from their only known culture source, the methanogenic Methanomassiliicoccales. Our results underline the diversity of archaeal membrane lipids preserved in wetlands and provide a baseline for the use of archaeal lipid distributions in wetlands as tracers of recent or ancient climate and biogeochemistry.

Keywords: temperature; pH; GDGTs; BDGTs; Me-GDGTs; crenarchaeol; isomers; Archaea; wetlands; biogeochemistry

Highlights

- IsoGDGT cyclisation is linked to pH/temperature, but controls are complex.

- The relative abundance of early/late-eluting isoGDGT isomers changes with pH.
- Early-eluting isoGDGT isomers can dominate (~70%) in near-neutral pH wetlands.
- BDGT producers, possibly methanogens, are likely selected for by near-neutral pH.
- Me-GDGTs distributions vary, reflecting changing sources/membrane adaptation.

1 Introduction

Wetland sediments are unique terrestrial archives that can provide insights into climatic and environmental change on land on both recent and geological timescales (Barber, 1993; Pancost et al., 2007; Huguet et al., 2010; Coffinet et al., 2015, 2018; Zheng et al., 2015; Naafs et al., 2018b; Inglis et al., 2019). They are also key components of the global carbon cycle, being the largest natural source of CH_4 to the atmosphere, a greenhouse gas with 25 times the warming potential of CO_2 on a centennial time-scale (Tian et al., 2015). In response to rising global temperatures, wetland CH_4 emissions are projected to increase by 33-60% by 2100 (Collins et al., 2013; Wania et al., 2013; Dean et al., 2018), acting as a positive feedback to anthropogenic climate change. Such methane emissions are ultimately driven by diverse archaeal assemblages with key roles in the processing of organic matter, notably mediating methanogenesis and the anaerobic oxidation of methane (AOM) (Cadillo-Quiroz et al., 2006; Zhu et al., 2012; Andersen et al., 2013; Bridgham et al., 2013; Segarra et al., 2015; Valenzuela et al., 2017).

Wetland environments preserve diverse archaeal lipid assemblages (Pancost and Sinninghe Damsté, 2003; Pancost et al., 2003; Weijers et al., 2004; Zheng et al., 2011; Naafs et al., 2018b, 2019; Yang et al., 2018) that have the potential to inform studies of archaeal-mediated carbon cycle-climate dynamics both in modern and ancient settings, and/or to be used as palaeoclimatic markers. In recent years an increasingly diverse suite

of archaeal core tetraether structures have been identified in environmental samples (including peat) (Liu et al., 2012, 2016; Naafs et al., 2018a) and cultures (Bauersachs et al., 2015; Becker et al., 2016), increasing the potential of lipid-focused chemotaxonomic and/or functional microbial studies and opening up novel avenues for proxy development. With a few notable exceptions (Weijers et al., 2004; Naafs et al., 2018b, 2018a; Yang et al., 2018), many of these compounds remain poorly characterised in wetland environments. Despite this, and unlike in other environments such as the open ocean (Schouten et al., 2002, 2013), the main environmental and ecological drivers of archaeal membrane lipid composition in wetlands - particularly with regards to core lipid types such as isoGDGT isomers and Me-GDGTs - are relatively poorly constrained. This contributes to an overall incomplete understanding of archaeal ecology and carbon cycling in wetlands, particularly in tropical regions, and the complex relationships of such microbial communities with climate and environmental change. In addition, it limits the interpretation of potentially informative lipid signatures in ancient sediments and other mesophilic settings.

The aims of this study are to examine the composition of archaeal lipids in three different types of modern wetlands, and to explore the ecological and environmental factors that drive differences in their distribution. We focused not only on the more widely studied isoGDGTs (De Rosa and Gambacorta, 1988; Schouten et al., 2013) and their chromatographically distinct earlier eluting isomers (Becker et al., 2013; Hopmans et al., 2016; Liu et al., 2016) but also examined the broader archaeal tetraether lipid distribution (Fig. S1 for structures) in our three main study sites. This includes i) butane-/pentane-dibiphytanyl glycerol tetraethers (B-/PDGTs) that have butanetriol or pentanetriol backbones instead of one of the more common glycerol moieties (Zhu et al., 2014;

Becker et al., 2016), ii) methyl-GDGTs (Me-GDGTs) that incorporate up to three additional methyl groups on their biphytanyl chain (Knappy et al., 2015), and iii) Me-GMGTs, which incorporate an extra methyl group on the biphytanyl chain as well as the covalent cross-link found in regular isoGMGTs (Knappy et al., 2014). GMGTs are a lipid class that were recently found to be abundant in some peats (Naafs et al., 2018a). We characterised both core lipids and the acid-hydrolysed core lipid derivatives of intact polar lipids (IPL-derived core lipids): IPLs are commonly used as markers for in situ, live microbial cells in the environment due to their relatively rapid degradation following cell lysis (White et al., 1979; Harvey et al., 1986; Lipp et al., 2008), although it has been shown that they can also be preserved over longer time-scales in some settings (Bauersachs et al., 2010; Logemann et al., 2011; Lengger et al., 2013, 2014; Xie et al., 2013). We focused in detail on three wetland sites, coming from Sebangau (Indonesia), the Florida Everglades (USA), and Tor Royal, Dartmoor (UK). These three sites constitute distinct wetland types with differing physicochemical and environmental characteristics. In addition, two of these sites are tropical wetland regions (i.e. the Florida Everglades and Sebangau, Indonesia), a poorly studied ecosystem type in terms of lipid geochemistry. As well as these three sites, we examine the composition of certain archaeal lipids (isoGDGT-0-4, their isomers and crenarchaeol) in our local sites as well as a globally distributed set of wetlands (Naafs et al., 2017), allowing for the identification and illustration of global patterns in archaeal lipid distributions. Collectively, this study provides insights into the environmental controls on archaeal lipid membrane regulation in mesophilic settings such as wetlands, and provides context for future studies utilising archaeal lipids to elucidate biogeochemical processes in modern and ancient wetlands.

2 Materials and Methods

2.1 Sites and Sampling

We primarily focused on three wetland sites. These were: Sebangau (Indonesia), Everglades (USA), and Tor Royal (UK). Site details are summarised in Table 1 (with additional details in Table S1). For each site, one core was analysed, though we recognise that peatlands are spatially heterogenous environments and therefore each core can only be considered partially representative of a particular wetland site.

Table 1: Geographical location and major physicochemical parameters of the three primary wetland sites.

Wetland	Country	Latitude	Longitude	Pore water pH	Mean Annual Air Temperature (°C)	Reference
Sebangau	Indonesia	02° 19' 16.96" S	113° 53' 54.29" E	3.2	26.2	Könönen et al., 2015; 2016
Tor Royal	United Kingdom	50° 32' 8.44" N	3° 58' 15.51" W	4.8	8.1	Collected for this study
Everglades	United States	26° 30' 18.00" N	80° 15' 52.00" W	6.8	23	Collected for this study

Sebangau National Park, Indonesia

The Sebangau peat swamp forest covers an area of around 5000 km^2 that forms the catchment of the Sebangau River around 200 km north of the Java Sea in south-central Borneo, Indonesia (Page et al., 1999, 2004). Peat accumulation in this region began around 26,000 cal. yr BP (Page et al., 2004). Whilst some logging occurred in the 1990s, a portion of undrained pristine swamp forest peat remains with a mixed tropical forest vegetation assemblage (Page et al., 2004; Sundari et al., 2012). Yearly average temperatures in the region are 26.2 °C, and precipitation is strongly influenced by El Niño/La Niña oscillations, averaging 2540 ± 596 mm per year (Sundari et al., 2012).

143 Rainfall occurs throughout the year, although there is a more pronounced wet-season
144 between November and April (Page et al., 2004).

145 A peat core measuring 1 m length was taken from a hollow in a section of
146 undrained swamp forest in March 2015 (02° 19' 16.96" S, 113° 53' 54.29" E) (as
147 detailed in Könönen et al., 2015, 2016 and at an elevation of around 18 m above sea-
148 level. The median water table depth at this site is 10.3 cm below the surface (Könönen
149 et al., 2015, 2016). The peat swamp forest is ombrotrophic and highly acidic with a
150 pH of 3.2 ± 0.3 recorded at time of sampling.

151

152 *Florida Everglades, USA*

153 The Florida Everglades covers around 6000 km^2 and is a predominantly freshwater
154 subtropical wetland in south Florida that has experienced peat accumulation for
155 approximately 4,000 years (Wright and Comas, 2016). Whilst the freshwater Florida
156 Everglades was originally a predominantly oligotrophic system, significant agricultural
157 run-off from the adjacent Everglades Agricultural Area during the 20^{th} and 21^{st} century
158 has increased nutrient levels in many areas, in particular towards the northern extent of
159 the wetland (Bae et al., 2015). Most rainfall occurs during the wet season (mid-May to
160 October), with an annual average of approximately 1400 mm (Wang et al., 2007). Mean
161 yearly temperature at a nearby weather station (Belle GL) is 23°C (Abtew et al., 2011).
162 In both oligotrophic and eutrophic areas of the Everglades, anoxic conditions tend to exist
163 at or near (~ 20 mm) the sediment surface, whilst SO_4^{2-} reduction and methanogenesis
164 are particularly enriched under eutrophic conditions (King et al., 1990; Castro et al.,
165 2004). Sulphate-rich water intrusion, primarily originating from agriculture, has been
166 shown to occur throughout the sampling area (Wang et al., 2007).

Sampling was conducted in May 2018 at the very end of the dry season, at a site in the north-east of Water Conservation Area One (WCA-1) within the Loxahatchee National Wildlife Refuge (26° 30' 18.00" N, 80° 15' 52.00" W), at an elevation of around 5 m above sea-level. The sampling area is dominated by Loxahatchee peat formed predominantly from water lily (*Nymphaea odorata*) remains (Wright and Comas, 2016). A 2 m peat/sediment core was collected with a Russian corer, and core-sections were immediately transported to a - 20 °C freezer at Florida Atlantic University (USA) before shipment on ice to the University of Bristol, UK, where they were sub-sampled and freeze-dried prior to lipid extraction. The water table was 36 cm above the peat surface at the time of sampling, remaining above the sediment surface all year-round at this site. The pH at the time of sampling was measured as near neutral at 6.8.

Tor Royal, UK

Tor Royal is a small domed mire situated at an altitude of 390 m within Dartmoor National Park, South-West UK. It is a designated Site of Special Scientific Interest due to its relatively pristine nature, which encourages the growth of many species of Sphagnum, ericaceous shrubs, sedges and grasses (Amesbury et al., 2008). Peat accumulation has occurred over the last ~6,000 years, with a maximum depth of 6.2 m (Charman et al., 1999). Based on a distinct change in the appearance and texture of the peat, the average water table depth was designated to be at ~ 30 cm below the surface. The average temperature in Princetown, 2 km to the north, is 8.1 °C (Burt and Holden, 2010). Rainfall is relatively consistent throughout the year, with an annual average precipitation of 2058 mm (Burt and Holden, 2010).

A core measuring 1 m length was collected in April 2018 with a Russian corer from the centre of the dome (50° 32' 8.44" N, 3° 58' 15.51" W), at an altitude of around 391 m. The core was immediately sub-sampled in the laboratory, before freeze-drying prior to analysis. Pore-water pH at time of sampling was measured as 4.8.

2.2 Lipid extraction

For the three new peat cores from the Indonesia, USA, and UK around 1.0 g of freeze-dried and homogenized peat was extracted using a modified Bligh-Dyer protocol (Bligh and Dyer, 1959). An aqueous phosphate buffer (pH = 7.2) was prepared through the addition of KOH pellets to a 0.5 M aqueous KH_2PO_4 solution. A monophasic mixture was subsequently made up containing methanol (MeOH), dichloromethane (DCM) and phosphate buffer (PB) in the ratio of 2:1:0.8 (MeOH:DCM:PB v:v). Subsequently, 16 ml of this extraction mixture was added to the freeze-dried sediment. The 16 ml g^{-1} mixture used is higher than that in used in many similar studies employing Bligh-Dyer extraction protocols in peat (e.g. 5 ml g^{-1} in Peterse et al., (2011) and 8 ml g^{-1} in Huguet et al., (2010)), since it has recently been demonstrated that higher solvent:sediment ratios maximise extraction efficiency of prokaryotic lipids, particularly in organic rich matrices such as wetland sediments or peat (see supplementary material of Chaves-Torres and Pancost, (2016). The solvent-sediment mixture was capped, ultrasonicated for 15 minutes, centrifuged at 3000 rpm for 12 minutes, and the supernatant was collected. This was repeated a total of 4 times and the supernatants were combined. The combined supernatants were adjusted to a final solvent ratio of 1:1:0.9 (MeOH:DCM:PB v:v) and the mixture was centrifuged at 2500 rpm for 10 minutes to separate the aqueous (MeOH and PB) and lower organic phase (DCM). This was repeated a total of 4 times, and the

organic phases were combined before being dried by rotary evaporation to yield the total lipid extract (TLE).

2.3 Processing of total lipid extract (TLE) for high performance liquid chromatography – mass spectrometry (HPLC-MS)

A glass column was packed with 1.5 g silica gel and pre-conditioned with Hex:EtAC (1:1 v/v). An aliquot of the TLE was loaded onto the column with a small amount of Hex:EtAC (1:1 v/v). Following the method of Lengger et al., (2013), core lipids (CLs) were eluted through with 8 ml of Hex:EtAC (1:2) and IPLs were eluted with 10 ml MeOH. Both fractions were dried under a gentle flow of N_2. In order to convert IPLs into their core lipid derivatives, the IPL fraction was heated with 5 ml of 5% methanolic HCl for 3 hours at 70 °C, cleaving polar head-groups and forming IPL-derived CLs. After allowing the solution to cool, 5 ml of double distilled water was added, and pH was adjusted to 4-5 using 1 M methanolic KOH. 5 ml of dichloromethane (DCM) was added, vortexed for 10 seconds, and the DCM phase was liquid-liquid extracted and collected in a separate vial. This was repeated 3 more times and the DCM extracts containing the IPL-derived CLs were combined before drying under a gentle stream of N_2. Both IPL-derived CL and CL fractions were then re-dissolved in hexane:isopropanol (Hex:IPA 99:1, v/v) and filtered using 0.45 μm PTFE filters (Thermo Fisher Scientific, Rockwood, TN, USA) before analysis.

2.4 HPLC-MS

CL and IPL-derived CL fractions were analysed separately. They were dissolved in 100 μl Hex:IPA (99:1 v/v) and 15 μl of this was injected and analysed by high performance

liquid chromatography / atmospheric pressure chemical ionisation – mass spectrometry (HPLC/APCI-MS) using a ThermoFisher Scientific Accela Quantum Access triple quadrupole mass spectrometer. As detailed by Hopmans et al., (2016), analyte separation was achieved in normal phase using two ultra-high performance liquid chromatography silica columns (1.7 μm, 2.1 x 150 mm). The column flow rate was 0.2 ml min^{-1} and compounds were eluted isocratically with eluent A (hexane:IPA 9:1 v/v) and eluent B (hexane): starting with 18% eluent A for 25 minutes, followed by a 55 minute gradient to 100% eluent A for 14 minutes, before decreasing to 18% in 5 minutes where it was held for a further 10 minutes. Selective ion monitoring (SIM) mode was used to improve sensitivity and reproducibility, targeting the protonated $[M+H]^+$ adducts of tetraether lipids at the following masses and at a scan time of 0.234 scans/s: m/z 1018, 1020, 1022, 1032, 1034, 1036, 1046, 1048, 1050, 1162, 1190, 1218, 1236,1240, 1242, 1244, 1246, 1290, 1292, 1294, 1296, 1298, 1300, 1302, 1310, 1312, 1314, 1316, 1318, 1328, 1330.

2.5 Additional analysis of samples from global peat database

In addition to data from the three newly collected peat cores, we analysed the archaeal core lipid distribution in a globally distributed set of peatlands (Naafs et al., 2017). Regular isoGDGT data from the global peat database was previously published (Naafs et al., 2018b) while the distribution of the isoGDGT isomers included here is novel. The global peat database is made up of 470 samples from 96 globally distributed peatlands, spanning a temperature range of - 8 to 27 °C and a pH range of between 3 - 8. Temperature data was generated for all sites via a bioclimatic model, PeatStash (Kaplan et al., 2003; Gallego-Sala and Prentice, 2013), whilst pH data is available for 52 of the 96

sites (Table S4). For full analytical details, please see Naafs et al., (2017). In short, the majority of samples were extracted using microwave extraction with 20 ml of dichloromethane:methanol (DCM:MeOH 9:1, v/v). The total lipid extract was re-dissolved in hexane:isopropanol (99:1, v/v), filtered using 0.45 μm PTFE filters and subsequently analysed via HPLC-APCI-MS, with the same conditions described in section 2.4 (though this time using m/z 1302, 1300, 1298, 1296, 1294, 1292, 1050, 1048, 1046, 1036, 1034, 1032, 1022, 1020, 1018, 744, and 653).

2.6 Statistical analysis

Hierarchical cluster analysis (HCA) was performed in R (RStudio v. 1.1.453; http://cran.r-project.org/) to examine the associations between different relative abundances of archaeal lipids identified in the three wetland sites and to explore the relationship between wetland environment and archaeal lipid composition. The hclust() function was used with a Euclidean distance metric (Jackson et al., 2009; Elling et al., 2017). In order to aid visualisation, when possible, samples were rearranged in depth order, providing this resulted in no fundamental change in grouping. Principal component analysis was also performed in R, using the same dataset as for HCA, to further examine variation and the relative weights of different lipid variables in driving clustering between our three sites and depths. Prior to PCA analysis, data was rescaled so that the mean = 0 and standard deviation was = 1. Canonical correspondence analysis (CCA) was also performed on a global dataset of specific archaeal lipid distributions. CCA is an ordination technique based on the chi-squared metric, widely applied to explore the ecological relationships between multiple 'species' variables (i.e. lipid relative abundances) and environmental variables (in this case pH and mean annual air temperature) (Braak and

Verdonschot, 1995; Jiang et al., 2014; Gong et al., 2015; Borcard et al., 2018). Following Borcard et al., (2018), we did not include compounds which were of very low relative abundance and absent in most sites (Cren' and isoGDGT-5), due to the potential 'many-zeros' skewing effect. Although some variation in pH and lipid abundance and distributions are expected with depth (Naafs et al., 2017), MAAT and pH were not resolved with depth in this dataset. Therefore, the site composition of lipids were averaged across several depths to perform CCA. As these are not weighted averages, they do not account for possible changes in absolute lipid concentrations with depth.

When required, a Shapiro-Wilk test was used to test for normality, with an alpha level of 0.05. Following this, unpaired t-tests and non-parametric Mann-Whitney significance tests were used for normally distributed and non-normally distributed data, respectively, when comparing differences in lipid biomarker composition between different sites and depths, with a cut-off value of $P < 0.05$.

3 Results

3.1 Occurrence and depth variation of CL and IPL archaeal lipids within three primary wetland sites

The relative abundance of individual compounds and classes varied both between and within the three sites. Whilst we characterised both IPL-derived and core lipids, the depth profiles of both lipid groups were similar, except where noted, and are therefore largely referred to collectively.

Lipids detected at our sites include characteristic archaeal membrane lipids such as the isoGDGTs, in particular isoGDGT-0, which despite varying in relative abundance among sites was generally the dominant archaeal lipid (average of 54% of total archaeal

lipids in both CL and IPL-derived pools in all sites). IsoGDGTs 1-4 were present at all sites but were much less abundant than isoGDGT-0 in the Everglades and Tor Royal. In Sebangau they were typically of a similar relative abundance as isoGDGT-0 (Fig. 1). Due to the consistently low abundance of crenarchaeol (which can contribute to m/z 1294), we did not correct the abundance of isoGDGT-4 for the abundance of crenarchaeaol in our samples. IsoGDGT-5, identified recently for the first time in mesophilic settings, including in other samples from the Sebangau wetland (Naafs et al., 2018b), was also present above detection limits here. It was absent in the Everglades and Tor Royal.

Based on their mass and relative retention time, nearly all samples contained earlier eluting isomers of isoGDGTs 1-4 (denoted isoGDGT-1'-4', Fig. 1), similar to that seen in other environmental samples (Pitcher et al., 2009; Becker et al., 2013; Hopmans et al., 2016; Liu et al., 2018; Sinninghe Damsté et al., 2018) and cultures (Sinninghe Damsté et al., 2018; Bale et al., 2019). Based on this data alone, the exact structural configuration of the isoGDGT isomers cannot be identified, although they could represent isomers with different ring stereochemistry (Becker et al., 2013; Sinninghe Damsté et al., 2018; Bale et al., 2019), or regioisomers with parallel or antiparallel glycerol arrangements (Becker et al., 2013; Liu et al., 2018, 2019).

In addition to these relatively common isoGDGTs and their isomers, several recently identified archaeal ether lipids were detected in our samples, with structures inferred from their relative elution time, characteristic $[M+H]^+$ ion, and comparison to previous studies. These included BDGTs with up to three cylopentane rings (Zhu et al., 2014; Meador et al., 2015; Becker et al., 2016), Me-GDGTs with up to two rings (Knappy et al., 2012, 2015; Zhu et al., 2014) and Me-GMGTs with up to two rings (Knappy, 2010; Yang et al., 2018) (Fig. 1).

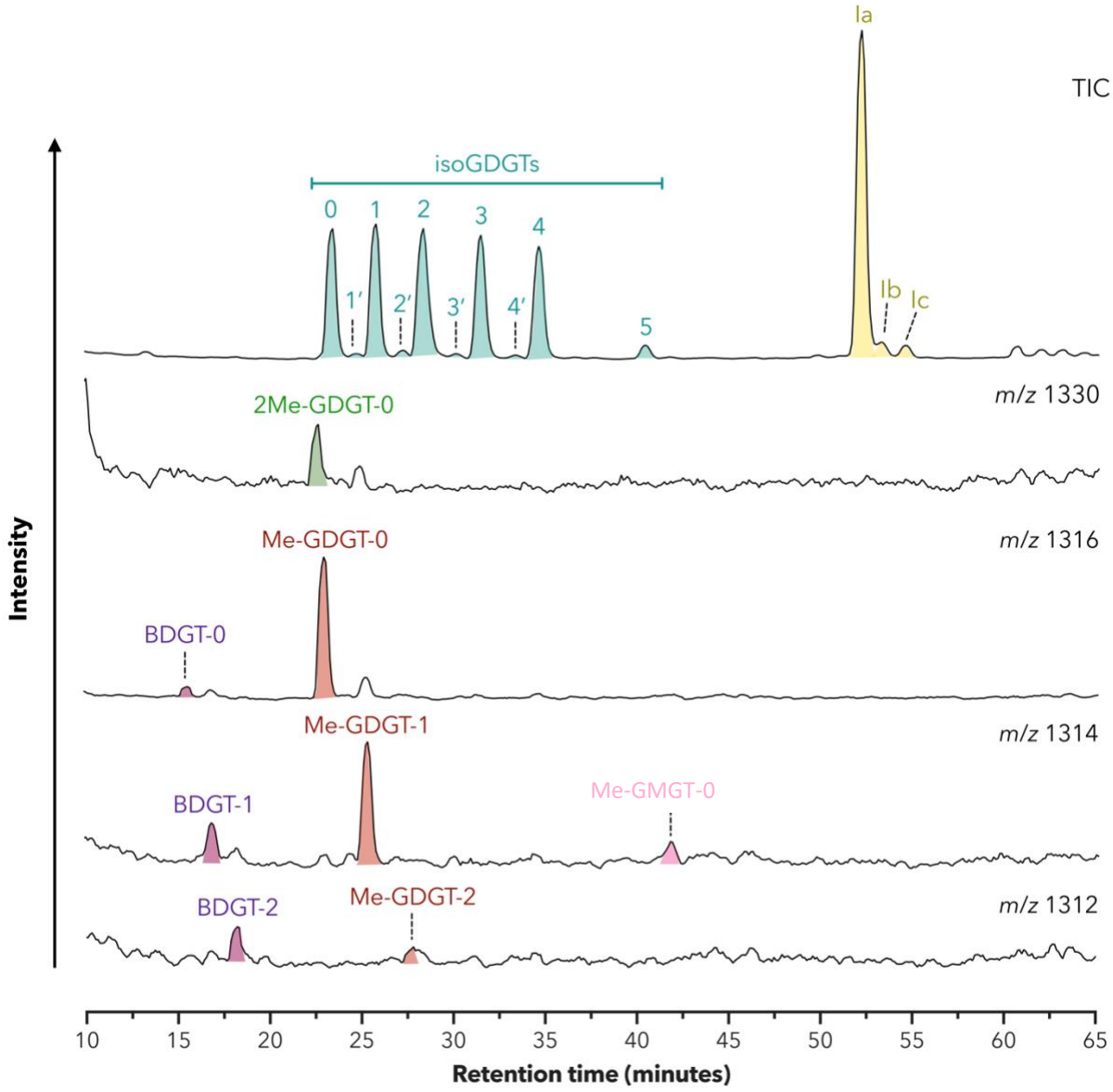

Figure 1. *HPLC-APCI-MS total ion chromatogram (TIC) and selected ion chromatograms of the tropical Sebangau wetland in Indonesia (37.5 cm depth), showing elution order of key archaeal compounds discussed in the text. isoGDGT isomers, which elute just before their respective cyclic isoGDGT, are distinguished from regular isoGDGTs by the presence of a prime symbol (′). Me-GDGTs typically elute ~ 0.25 minutes prior to their isoGDGT homolog, whilst 2Me-GDGTs elute ~0.5 minutes prior to their respective isoGDGT. Compounds Ia-c represent bacterial branched brGDGTs (Sinninghe Damsté et al., 2000) which are not the focus of this study.*

We visualise and analyse the compositional differences between different sites and depths in detail via hierarchical cluster analysis below, but briefly summarise the depth

behaviour of key compounds here. BDGT abundances relative to those of isoGDGT-0 increased in the catotelm (the deeper, permanently waterlogged and anoxic part of the peat column) of Sebangau and Tor Royal, and at depth in the Everglades, which is likely anoxic throughout (King et al., 1990; Castro et al., 2004). IPL-derived BDGTs made up a higher relative abundance of the total IPL-derived archaeal lipids than in the core lipids and increased at depth particularly in this fraction (Fig. 2a-c). PDGTs exhibit similar increases in abundance relative to the BDGTs with depth in all sites (Fig. 2d-f). The relative abundance of Me-GDGTs also increased with depth in Sebangau, whilst staying relatively stable in Tor Royal and the Everglades. In contrast, Me-GMGTs increased substantially in relative abundance below the acrotelm-catotelm boundary in Sebangau and Tor Royal, with only a minor increase with depth in the likely permanently anoxic Everglades core (Fig. 2j-i). Crenarchaeol and its isomer (Cren'; Fig. 2m-o), which were present in very low abundances in all sites, decreased with depth progressively in both IPL-derived and CL fractions of Sebangau. In both Tor Royal and the Everglades, the relative abundances of Crenarchaeol and Cren' showed no clear downcore trend, although concentrations were just above the detection limit in these peats, potentially obscuring subtle downcore trends.

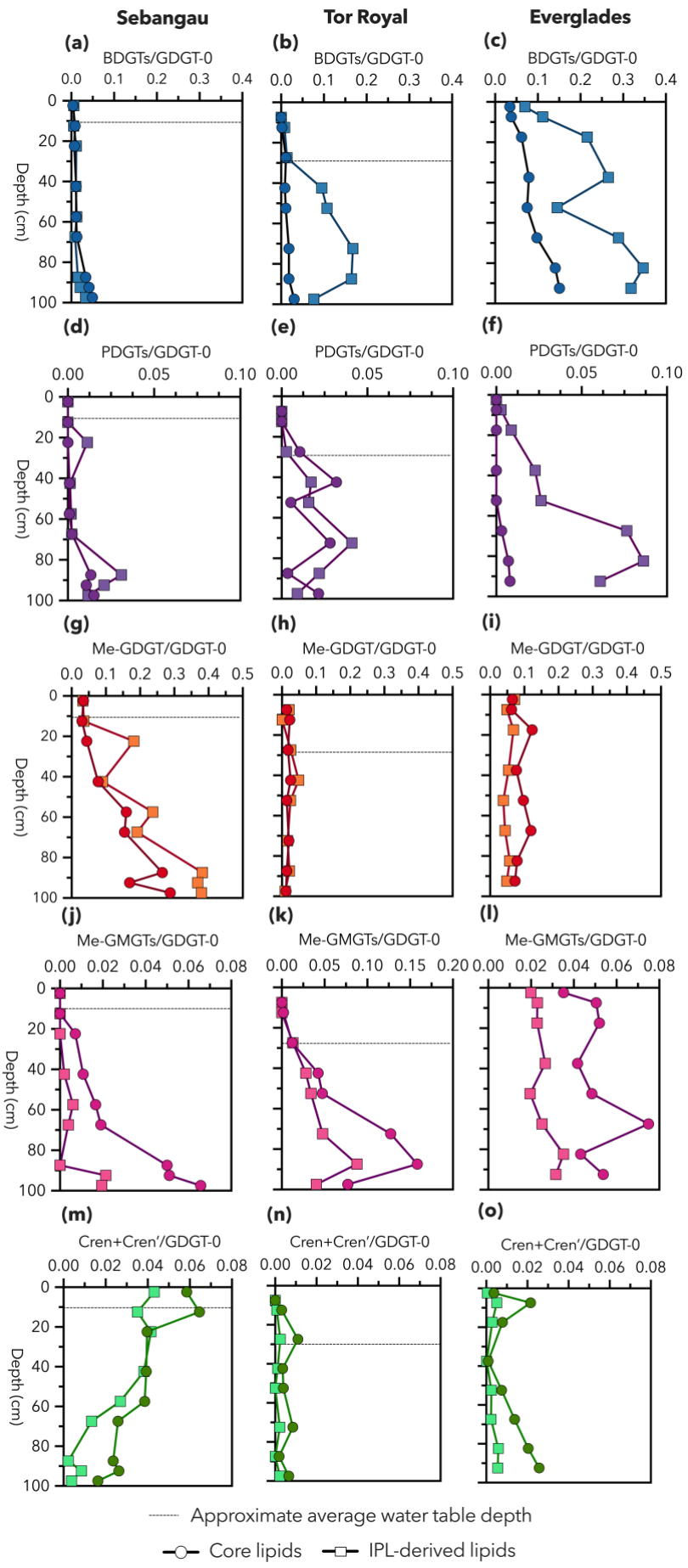
Sebangau
Tor Royal
Everglades
(a)
(b)
(c)
BDGTs/GDGT-0
0.0 0.1 0.2 0.3 0.4
(d)
(e)
(f)
PDGTs/GDGT-0
0.00 0.05 0.10
(g)
(h)
(i)
Me-GDGT/GDGT-0
0.0 0.1 0.2 0.3 0.4 0.5
(j)
(k)
(l)
Me-GMGTs/GDGT-0
0.00 0.02 0.04 0.06 0.08
0.00 0.05 0.10 0.15 0.20
(m)
(n)
(o)
Cren+Cren'/GDGT-0
0.00 0.02 0.04 0.06 0.08
Depth (cm)
0 20 40 60 80 100
Approximate average water table depth
Core lipids
IPL-derived lipids

Figure 2. *Depth profile of key archaeal compounds, relative to isoGDGT-0, in the three principal wetland sites. A dotted line denotes the approximate position of the acrotelm-catotelm boundary, whilst the core lipid and IPL-derived lipid pools are shown by circles and squares respectively. Note the average water table depth in the Everglades site is above the peat surface.*

3.2 Variation in relative abundance of archaeal lipids between sample sites and depths

We performed hierarchical cluster analysis (HCA) on both the IPL-derived (Fig. 3) and CL fractions (Fig. S2). Both IPL-derived and CL fractions showed near-identical partitioning in HCA. We performed this alongside a principal component analysis on the same dataset (Fig 3B) which we address below. For both the HCA and PCA, we predominantly focused on IPL-derived lipids below; even when accounting for long term preservation of certain IPLs (Lengger et al., 2013; Chaves-Torres and Pancost, 2016), these more likely reflect the actual distribution of live biomass than their core lipid counterparts (Harvey et al., 1986; Lipp and Hinrichs, 2009; Buckles et al., 2013).

Author's preprint copy for article published in *Organic Geochemistry*
(https://doi.org/10.1016/j.orggeochem.2020.104080)

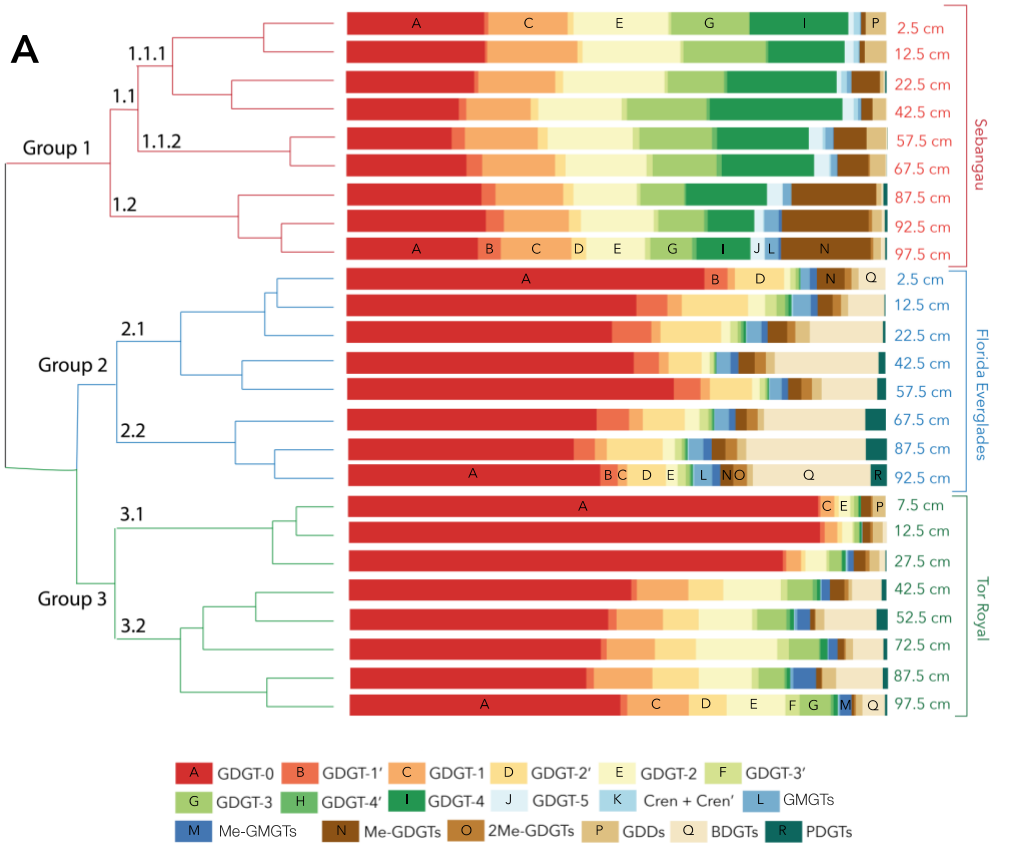

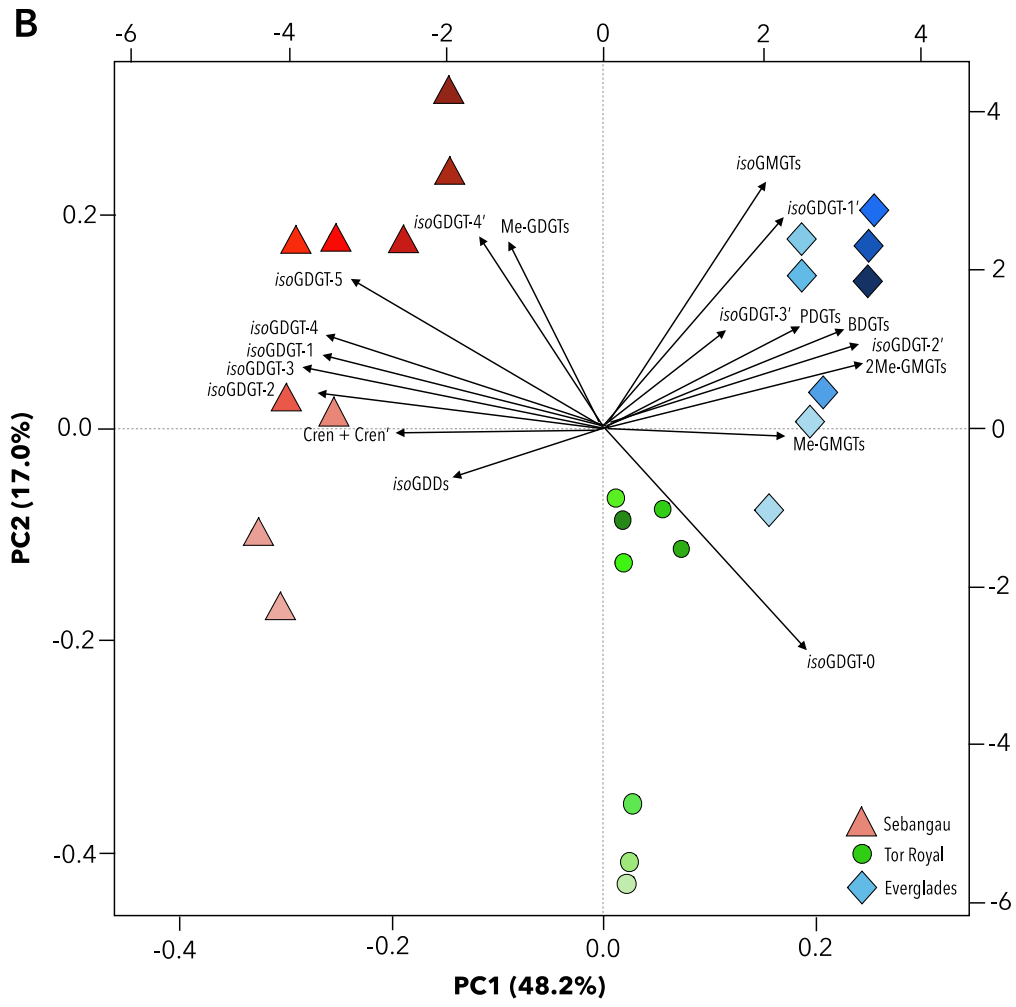

Figure 3. *Panel A shows a hierarchical cluster analysis (HCA) dendrogram of the IPL-derived archaeal lipid fractions in our three wetland sites, with relative proportion bar-plots illustrating the relative proportion of different archaeal lipid groups. An analogous figure for CLs can be found in the supplements (Fig. S2). Where possible, in the upper and lowermost samples of each site, bars are labelled with a letter corresponding to the key. Panel B shows a principal component analysis biplot for the same set of archaeal lipid relative abundances in Sebangau (Indonesia), Tor Royal (UK), and Everglades (USA). Points represent different depths within each site, with darkening shades of sample points corresponding to progressively deeper samples within a site (e.g. light red represents shallow samples from Sebangau, whilst darker red corresponds to deeper samples from the same site). See Table S3 for loadings.*

In the IPL-derived lipids, the data clustered into three groups, exclusively defined by wetland site: Sebangau (group 1), Florida Everglades (group 2) and Tor Royal (group 3). The CLs partitioned in the same way with only one exception: the sample from 2.5 cm in the Everglades clustered within the same group as samples from Tor Royal, most likely driven by the high relative abundance of isoGDGT-0 in this particular sample (Fig. S2), which was similar to that of the shallow samples in Tor Royal.

Samples from Sebangau (group 1) have a characteristic distribution in which isoGDGTs-1-4 are of a comparable abundance to isoGDGT-0 (24% ± 2%), with isoGDGT-4 particularly enriched in Sebangau relative to the other groups. In comparison, both the Florida Everglades (group 2) and Tor Royal (group 3) are characterised by higher isoGDGT-0 proportions (52 % ± 8 % and 61 % ± 20 % average respectively). Sebangau also has the lowest relative abundances of isoGDGT-1' to -4' isomers. In order to illustrate these differences in the relative abundance of the early and late eluting isoGDGT isomers between different sites, we calculated the following ratio for each sample. We chose to exclude the isoGDGT-4 isomers from the calculation in order to enable comparison of the ratio with other wetland sites in which isoGDGT-4 and its isomer are not present above detection limits:

410 $$isoGDGT_{Isomer\ Index} = \frac{\sum_{1'}^{3'} isoGDGT}{\sum_{1'}^{3'} isoGDGT + \sum_{1}^{3} isoGDGT}$$

411

412 The averaged isoGDGT$_{Isomer\ Index}$ ratio for core lipids in Sebangau was 0.09 ± 0.04.
413 Tor Royal and the Everglades had ratios of 0.26 ± 0.08 and 0.72 ± 0.06, respectively.
414 This ratio is plotted against depth for each site in Figure 4. Both core lipids and IPL-derived
415 lipids had similar depth profiles, varying downcore and with a higher ratio deeper in the
416 core, particularly for CLs in the Everglades.

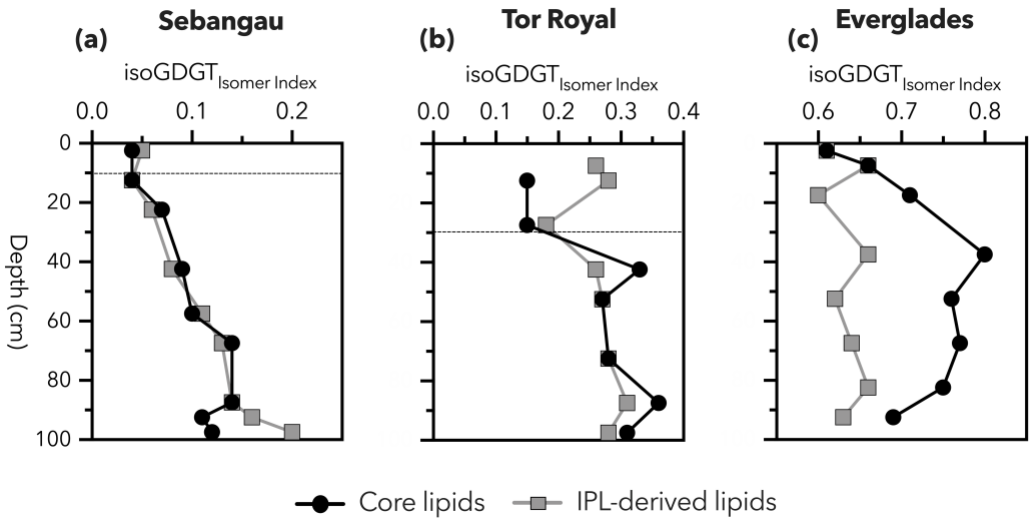

417

418 ***Figure 4.*** *Depth profile of isoGDGT$_{Isomer\ Index}$ in the 3 primary wetland study sites. A dotted*
419 *line denotes the approximate position of the acrotelm-catotelm boundary, whilst the core*
420 *lipid and IPL-derived lipid pools are shown by circles and squares respectively. Note the*
421 *average water table depth in the Everglades site is above the peat surface.*
422

423 Both the Everglades and Tor Royal contain elevated proportions of BDGTs compared to
424 Sebangau: making up 15 % ± 7 of total lipids in the Everglades and 4 % ± 4 % of total
425 lipids in Tor Royal. The Florida Everglades are also characterised by relatively abundant
426 PDGTs, particularly at depth (~ 2 % ± 2 %, as opposed to < 1.0 % in Tor Royal and
427 Sebangau).

The samples did further cluster by depth within our HCA analysis, but only within their particular geographic locality, suggesting that depth (reflecting redox conditions) is a secondary control on the archaeal lipid composition; that is to say that samples from the same depth in different wetlands do not have systematically similar compositions. For example, in the IPL-derived lipids of Sebangau (Fig. 3a), samples split into three distinct depth groups, from between 2.5 cm – 42.5 cm (group 1.1.1), 57.5 cm – 67.5 cm (group 1.1.2), and 77.5 cm – 97.5 cm (group 1.2). These three groups were primarily characterised by increasing relative abundances of Me-GDGTs, making up 2 % ± 2 % of total archaeal lipids in shallow group 1.1.1, 6 % ± 0.5% in intermediate group 1.1.2, and 16 % ± 0.5% in deep group 1.2.

Despite anoxic conditions existing throughout the sediment profile of the Everglades, archaeal lipid compositions also show clear vertical zonation: samples from the top 52.5 cm (group 2.1) clustered separately from those from the bottom 25 cm (i.e. 67.5 cm – 92.5 cm; group 2.2). Shallow group 2.1 was predominantly characterised by lower relative abundances of BDGTs (11 % ± 6 %) and PDGTs (0.7%) than in the deep group 2.2: 19 % ± 3 % ($p = 0.0364$) and 3 % ± 0.5% ($p = 0.0008$), respectively.

Tor Royal also showed clear depth-zonation; group 3.1 contains only samples from within the oxic acrotelm, whilst group 3.2 is made up uniquely of samples from the anoxic catotelm. This is mainly driven by differences in the relative abundance of isoGDGT-0: group 3.1 (2.5 cm – 27.5 cm) is characterised by a significantly higher average relative isoGDGT-0 abundance of 86 % ± 4 %, whilst those in catotelm group 3.2 (42.5 cm – 97.5 cm) have average isoGDGT-0 abundance of 47 ± 3 % ($p = 0.0357$). In addition, acrotelm group 3.1 has a very low relative abundance of Me-isoGMGTs and BDGTs (<1%), with

451 both compound classes increasing significantly in catotelm group 3.2 (2% ± 1% and 7 %
452 ± 2 % respectively).

453 However, it must be noted that the effect of changes in redox state on the total
454 archaeal lipid assemblage is likely underestimated in this HCA, as we treat each individual
455 isoGDGT as an individual variable rather than grouping archaeal isoGDGTs into one
456 class. Grouping them into one class removes the effect of temperature and pH on
457 isoGDGT distribution. Indeed, when individual isoGDGTs are assimilated into one
458 compound class and HCA variable, the strength of clustering between the different
459 wetland localities is slightly weakened with deeper samples from Sebangau and Tor Royal
460 instead occupying the same cluster. This suggests that – at least in terms of the relative
461 proportion of different compound classes – depth (potentially redox state) also exerts a
462 strong influence on archaeal lipid assemblage, alongside pH and temperature.

463 As above, we further ran a principal component analysis (PCA) on the same data
464 as for the HCA, in order to further elucidate differences in archaeal lipids between our
465 three primary sites, and to gain a more quantitative understanding of the relative weight
466 of lipid variables in determining clustering (Fig. 3B and Table S3 for loadings on PC1 and
467 PC2). When considering the relative abundance of IPL-derived lipids, the first two
468 principal components explained 65.2% of the total variance (Fig. 3B). Consistent with
469 HCA, the samples were split into clusters that generally corresponded to individual
470 wetland sites. Also largely consistent with the results from HCA, depth generally affected
471 clustering, but only within sites rather than systematically across all sites, with shallower
472 and deeper samples generally clustering separately within their site-clusters. isoGDGT-
473 1-5 and Me-GDGTs were negatively associated with PC1, representing lipids that were
474 more abundant in the acidic, tropical Sebangau site. Positive scores on PC1 therefore

likely reflect an increase in pH. isoGDGT-1'-4', isoGMGTs, BDGTs, PDGTs and 2Me-GDGTs were positively associated with PC2, representing lipids that were particularly abundant in the tropical, higher pH Everglades site. isoGDGT-0 was strongly negatively associated with PC2, and was particularly abundant in shallower Tor Royal samples. Higher scores on PC2 could possibly reflect increasing temperature or depth, although more data, particularly in colder regions, would be required to explore this further.

3.3 Globally-resolved analysis of isoGDGT distributions via Canonical Correspondance Analysis

We chose to use the widespread and widely-studied isoGDGTs to place our three primary study sites within a global context, and to further deconvolve the relationships between pH, temperature and the distribution of archaeal membrane lipids in peat. To do this we conducted a canonical correspondence analysis (CCA) algorithm (Braak and Verdonschot, 1995) using the vegan 2.3-1 package in R, following Borcard et al., (2018) (Fig. 5) (Oksanen et al., 2017). We performed this analysis on sites from the global database of wetland core lipid distributions generated by Naafs et al., (2017, 2018b) for which both pH and temperature measurements were available (Table S6), as required for CCA, as well as our three additional study sites (Fig. 5) (n = 55). Low Variance Inflation Factors (VIFs) of <2 for both pH and temperature demonstrate an absence of collinearity, as required for CCA (Borcard et al., 2018). We used ANOVA (999 permutations) (using the anova.cca function) to test (a) the overall significance of the CCA model, (b) the significance of each environmental variable and (c) the significance of the CCA1 and CCA2 axes. All were found to be significant ($p = < 0.005$). In order to aid visualisation of

499 our CCA biplot (Fig. 5), we sub-divided the data into four wetland 'end-member'
500 categories, broadly representing different wetland temperature and pH regimes. It must
501 be stressed that these categories were chosen to aid illustration in our CCA analysis,
502 rather than reflecting real-world thresholds. We note that other compounds which we
503 discuss in later sections (e.g. BDGTs and Me-GDGTs) likely vary widely in response to
504 changing environmental conditions and may therefore represent key differences between
505 wetlands, as suggested by our three primary study sites. Therefore, although not included
506 here, future studies should build on these findings and focus on exploring their variability
507 on a similar global scale.

508 The clustering of sites belonging to each wetland type category in our CCA
509 analysis illustrates the effect of the chosen environmental parameters on archaeal lipid
510 composition on a global scale. The three in depth study sites – Sebangau, Tor Royal and
511 the Everglades – broadly cluster with other sites in the global database (Fig. 5) also
512 assigned to their temperature/pH category, suggesting that – at least in terms of the
513 relative abundance of the compounds in this analysis – they can be considered
514 representative for their particular wetland type. In this CCA (Fig. 5), the position of each
515 lipid corresponds to its ecological optimum in relation to the respective temperature and
516 pH gradients (shown by arrowed lines). This means that possible relationships between
517 species variables (i.e. lipids) and environmental variables (i.e. temperature and pH), often
518 not visible in 2-dimensional property:property space, can be elucidated (Pearson et al.,
519 2008). To summarise what is shown in Figure 7: the relative abundance of isoGDGT-0
520 was most closely associated with the lower MAAT cluster containing Tor Royal, whilst
521 cyclic isoGDGTs, in particular isoGDGT-3 and -4, were most closely associated with
522 acidic and high MAAT wetlands, including Sebangau. These results from the global

database replicate trends observed in our primary three sites. Interestingly, isoGDGT-1'-3' isomers showed opposing behaviour to their later eluting isoGDGT isomers, being most closely associated with higher pH wetlands, such as the Florida Everglades (where early-eluting isomers make up ~ 70% of all isoGDGTs 1-3). Crenarchaeol was most closely associated with more alkaline wetlands.

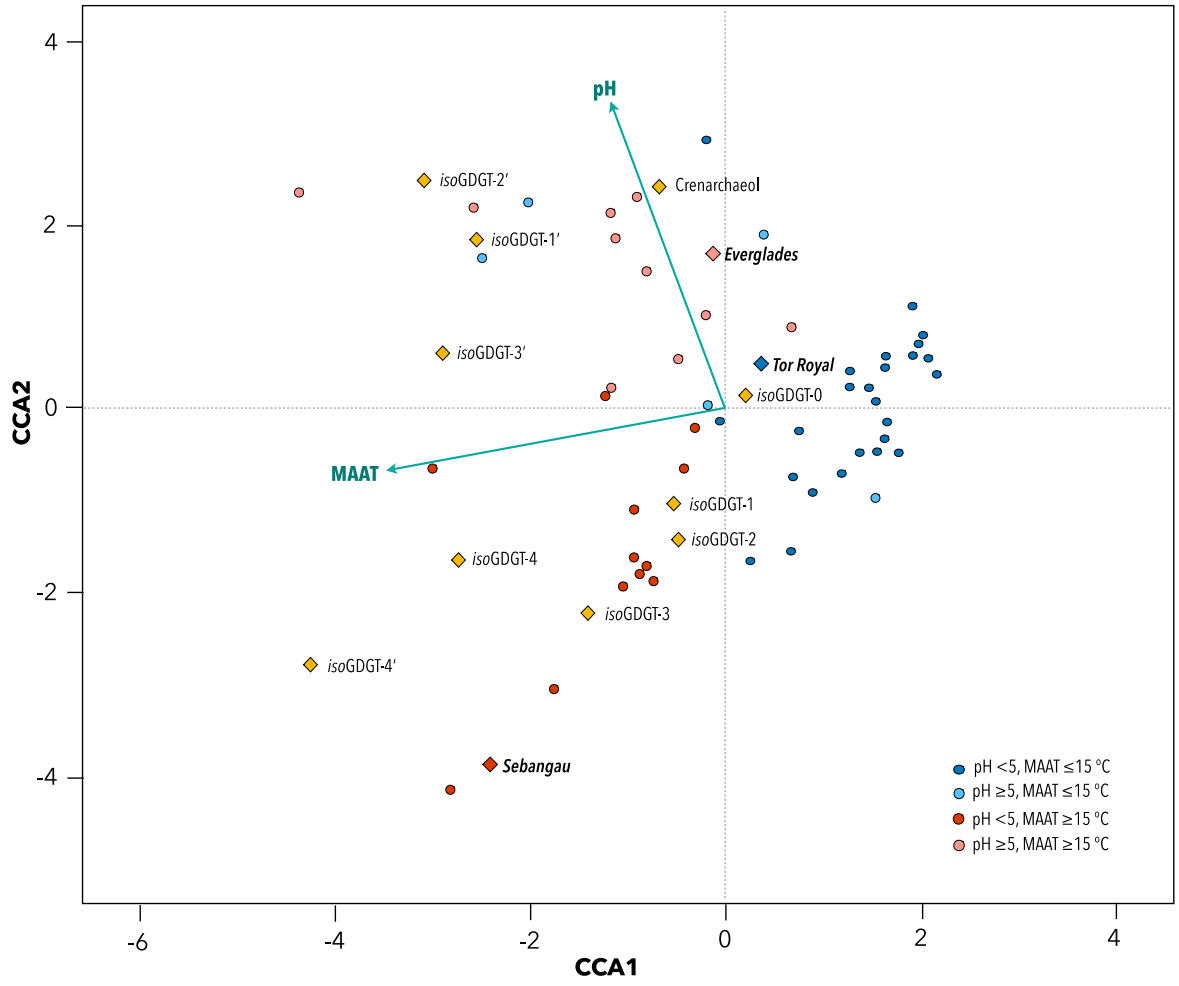

Figure 5. *Canonical correspondence analysis biplot showing study sites (averaged composition across core) and a subset of peat database samples from Naafs et al., (2017) (See Table S6). This subset corresponds to localities in the database for which both temperature and pH metadata are available (a necessary condition of CCA). In this CCA, the position of each lipid corresponds to its ecological optimum in relation to the respective temperature and pH gradients (shown by arrowed lines). Sites have been placed in categories (see key) in order to illustrate the impact of different temperature regimes and physicochemical conditions (pH) on sample composition. These categories represent arbitrary boundaries in mean annual air temperature and pH, and aim to aid interpretation rather than representing real-world threshold conditions.*

In the following sections we couple findings from this CCA with insights from our three main sites to explore the relationships of these archaeal lipids with temperature, pH and depth. This lipid-focused study provides constraints on the present-day global distribution of Archaea in wetland sediments and provides insights into how archaeal communities moderate their lipid biochemistry in response to their external environment.

4 Discussion

The relatively low taxonomic specificity of most archaeal lipids (de Rosa et al., 1986; Schouten et al., 2013; Bauersachs et al., 2015; Elling et al., 2017) makes it challenging to directly assign specific sources to compounds in environmental samples. This is made more challenging by the high diversity of archaeal communities in wetlands (Cadillo-Quiroz et al., 2008; Narrowe et al., 2017) and the likelihood of a significant input from uncultured phyla for which lipid compositions are not known. For example, the uncultured phylum Bathyarchaeota (formerly Miscellaneous Crenarchaeotal Group) can in some cases be the most abundant archaeal taxa in wetlands (Narrowe et al., 2017; Bai et al., 2018), but their membrane composition is unknown and so their contribution cannot be easily assessed.

Several decades of culture and incubation experiments (De Rosa et al., 1980; Uda et al., 2001; Wuchter et al., 2004; Schouten et al., 2007; Boyd et al., 2011) together with data from a range of environments (Schouten et al., 2002; Pearson et al., 2008; Yang et al., 2016; Naafs et al., 2018b) and biophysical and computational molecular dynamic studies (De Rosa et al., 1994; Chong et al., 2005, 2012; Shinoda et al., 2005; Chugunov et al., 2014; Caforio and Driessen, 2017; Huguet et al., 2017), predominantly focusing

563 on the degree of cyclisation of isoGDGTs, have shown that Archaea modify their
564 membrane compositions in order to maintain fluidity in response to changes in
565 extracellular pH and temperature. Differences between the composition of archaeal lipids
566 in different wetlands are therefore the product of both differences in archaeal community
567 and that community's adaptation to extracellular conditions, integrating both
568 accumulating in situ community production but also input from the time of deposition at a
569 given depth interval.

570 It is important to stress that we focus on relationships with pH and temperature,
571 but other variables that we have not measured (e.g., electron donor flux and energy
572 availability) can also control archaeal lipid distributions (Elling et al., 2014, 2015; Qin et
573 al., 2015; Hurley et al., 2016; Evans et al., 2018; Zhou et al., 2020). Additionally, pH in
574 particular is a 'master-variable', regulating other important geochemical characteristics
575 in wetlands which we do not directly measure such as nutrient speciation and
576 concentration. However, pH has been shown to be the main determining variable for soil
577 archaeal community composition and diversity, even between tropical and temperate
578 biomes (Tripathi et al., 2015), although climatic factors including temperature are
579 important additional determinants of microbial community composition (Delgado-
580 Baquerizo et al., 2018).

581 Our three main study sites each have a unique lipid fingerprint, with clear
582 variations between sites but also across redox boundaries (Fig. 2 - Fig. 3). This provides
583 possible insights into both the ecology of various lipid source-organisms, and/or their
584 membrane lipid adaptation to the measured environmental conditions. In the following
585 sections, we begin by discussing the isoGDGTs, their isomers and crenarchaeol,
586 contextualising our observations from our three main sites with a database of global

wetlands generated by Naafs et al., (2017) to examine the parallels between our local observations and those of wetlands globally. Finally, we discuss the distributions of Me-GDGTs and Me-GMGTs, BDGTs and PDGTs in our three primary sites.

4.1 IsoGDGTs, isoGDGT isomers and Crenarchaeol

Regular isoGDGTs and crenarchaeol are the most widely studied archaeal lipids, nearly ubiquitous and the most abundant archaeal membrane lipids in most environments (Schouten et al., 2013). Previous work has shown that the degree of cyclisation of isoGDGTs is influenced by temperature and pH (De Rosa et al., 1980; Schouten et al., 2002; Pearson et al., 2008; Sinninghe Damsté et al., 2012a; Qin et al., 2015; Yang et al., 2016). This appears to be supported by the data from our three study sites with higher proportions of isoGDGTs-1-4 at the tropical Sebangau peatland. However, in a previous analysis of the global dataset of peatlands, no clear relationship between ring index (or TEX_{86}) and temperature was found (Naafs et al., 2018b) (see below). Crenarchaeol abundances in wetlands appear to be governed by pH but also aridity via its influence on redox conditions (Zheng et al., 2015, 2018; Naafs et al., 2019), consistent with the largely aerobic ammonia oxidising ecology of its Thaumarchaeota source (Pester et al., 2011). There is little known about the controls on the abundance and distribution of isoGDGT isomers in wetlands.

4.1.1. Distinct differences in isoGDGT distribution in global wetlands in response to temperature and pH

The distribution of isoGDGTs is highly variable between different sites and climatic and physicochemical regimes. The tropical and acidic site Sebangau is characterised by

611 a distinct distribution in which the abundances of isoGDGTs-1 to -4 are similar to
612 isoGDGT-0 (Fig. 1 and 3a). Other acidic and high temperature wetland sites share this
613 relative enrichment in the abundance of isoGDGT-1 to -4 as demonstrated by their
614 behaviour in our CCA analysis (Fig. 5). This distribution pattern is similar to that of
615 isoGDGT distributions found in acidic and high temperature terrestrial hot springs
616 (Pearson et al., 2008), with the slight dominance of isoGDGT-4 amongst the cyclic
617 isoGDGTs also reminiscent of the distribution in (hyper)thermophilic Archaea (Uda et al.,
618 2001; Sinninghe Damsté et al., 2012b). This observation is consistent with archaeal
619 membrane adaptation in acidic and high temperature environments: that is, the presence
620 of cyclopentane rings on the isoGDGT core lipid increases membrane impermeability to
621 protons, whilst also limiting the rotational freedom of the chain helping to maintain
622 appropriate membrane fluidity and stability (Dannenmuller et al., 2000; Gabriel and Lee
623 Gau Chong, 2000; Caforio and Driessen, 2017). These findings are consistent with the
624 recent identification of isoGDGT-5 – a lipid previously thought to be restricted to Archaea
625 inhabiting extremophilic environments – in acidic and tropical wetlands with a pH of < 5.1
626 and a mean annual air temperature > 19.5 °C (Naafs et al., 2018b).

627 Whilst our multivariate data show a clear link between cyclic isoGDGTs and
628 acidic/higher temperature wetlands, recent work on the same dataset of globally
629 distributed wetlands as used in this study showed no clear correlation with either pH or
630 temperature with TEX_{86} or the Ring Index (Naafs et al., 2018b), two established molecular
631 ratios which reflect the degree of cyclisation of isoGDGTs. This has also been observed
632 for hot-spring environments, where neither index directly correlates with pH or
633 temperature (Pearson et al., 2004), though a link between cyclic isoGDGTs and low pH
634 or high temperatures is shown when multivariate methods, which take into account the

635 effect of both temperature and pH, are applied (Pearson et al., 2008). The lack of a clear
636 relationship is likely compounded in wetlands by their relatively high archaeal diversity,
637 encompassing inputs from several cultured and uncultured phyla (Pazinato et al., 2010;
638 Narrowe et al., 2017) with differing ring-temperature (and pH) relationships. This is in
639 contrast to open ocean environments, where planktonic Thaumarchaeota are purported
640 to be the dominant source (Weijers et al., 2011; Elling et al., 2015; Besseling et al., 2018)
641 and a clear relationship with temperature exists (Schouten et al., 2002). In addition,
642 wetlands are highly heterogenous systems, with sharp gradients in geochemical
643 parameters occurring over small spatial scales that can dramatically alter archaeal
644 communities (Narrowe et al., 2017). This is particularly important as several studies in
645 recent years have demonstrated that environmental parameters other than temperature
646 and pH can also affect isoGDGT cyclisation in Archaea (Elling et al., 2014, 2015; Qin et
647 al., 2015; Hurley et al., 2016; Evans et al., 2018), likely further clouding the ring-
648 temperature or ring-pH relationships. Nonetheless, our multivariate analysis
649 demonstrates that the isoGDGT distribution, and especially ring number, is responsive to
650 changes in temperature and pH on a global scale in terrestrial mesophilic settings,
651 consistent with previous work showing that isoGDGTs in soils correlate with temperature
652 in local-scale altitudinal transects (Yang et al., 2016).
653
654 ### 4.1.2 isoGDGT isomers respond to pH in global wetlands
655 Analytical developments in the last two decades have revealed the existence of several
656 isoGDGT isomers in environmental samples and culture (Sinninghe Damsté et al., 2002;
657 Sinninghe Damsté et al., 2012; Becker et al., 2013; Liu et al., 2018). Theoretically,
658 isomerism in isoGDGT core lipid structures can arise in several ways, and are discussed

659 in detail in Becker et al., (2013). Possible differences include (a) regioisomeric differences
660 in the configuration of the two glycerol units, which can be parallel or anti-parallel to each
661 other (Grather and Arigoni, 1995; Becker et al., 2013; Liu et al., 2018, 2019); (b)
662 structural differences in the position of the ring(s) on the biphytane moieties (Becker et
663 al., 2013) and; (c) differences in cyclopentane ring stereochemistry (Becker et al., 2013;
664 Sinninghe Damsté et al., 2018; Bale et al., 2019). Based on HPLC-MS data alone, it is
665 not possible to detect the configuration of the isoGDGT isomers present in the wetlands
666 in this study.

667 Both core lipids and IPL-derived lipids generally show relatively minor increases in
668 the $isoGDGT_{Isomer\ Index}$ ratio with depth in all three sites (except in the CLs in the perennially
669 anoxic Everglades; Fig. 4), possibly representing changing archaeal communities with
670 depth or adaptation to changing growth conditions. Clear differences in the relative
671 abundance of these isomers do exist between different sites: the higher pH Everglades
672 study site is characterised by a dominance of early eluting isoGDGT isomers compared
673 to the later eluting isoGDGTs and a high $isoGDGT_{Isomer\ Index}$, in contrast to the low pH
674 Sebangau site in which they are almost absent, and the moderate pH Tor Royal where
675 they occur in low abundances (Fig. 3a). CCA suggests similar relationships exist globally
676 (Fig. 5). Scatterplots (Fig. 6) demonstrate that the $isoGDGT_{Isomer\ Index}$ is moderately and
677 significantly correlated with pH, although, based on these, no clear relationship with
678 temperature exists.

679 Whilst the precise taxonomic or physiological significance of these isomers
680 remains unknown, the correlation with pH is also consistent with a previous study
681 analysing isoGDGT distributions in soils immediately adjacent to two terrestrial hot
682 springs, in which the early eluting isomers of GDGT-1 and GDGT-2 were present in larger

proportions in the more alkali hot-spring soils (Pitcher et al., 2009). Moreover, a recent culture study on the Thaumarchaeota *Ca.* Nitrosotenuis uzonensis also showed increases in the relative proportion of early eluting isomers with increasing temperature (Bale et al., 2019). Whilst there is no such clear relationship with temperature within our datasets, the results of this previous study do demonstrate that changes in isoGDGT$_{\text{Isomer Index}}$ could concur a physiological advantage to certain Archaea under evolving growth conditions, as may be the case with changing pH in wetlands.

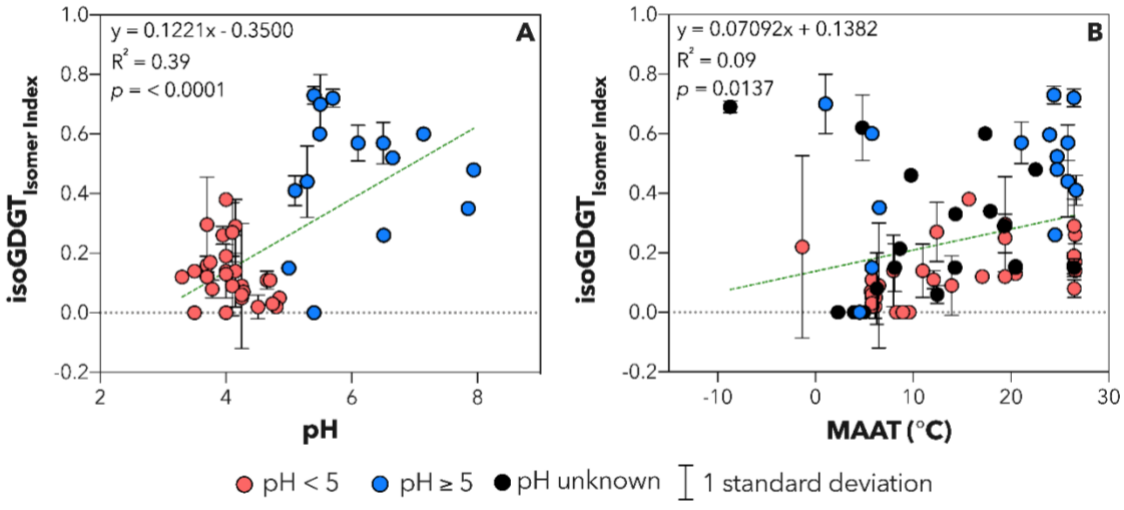

Figure 6. *isoGDGT$_{\text{Isomer Index}}$ plotted against pH (A) and temperature (B). See S6 for data.*

However, at present, it is not possible to tell whether our observations correspond to an archaeal membrane homeostasis mechanism, or rather whether they are a taxonomic signal caused by broad changes in archaeal community in different environments. Previous work argued that changes in the relative abundance of Thaumarchaeota versus AOM-related archaeal communities, could possibly drive differences in regioisomerism in marine settings (Liu et al., 2019). This specific change in archaeal community likely does not underly our observations, since crenarchaeol (see Section 4.1.3) is consistently found in very low abundance in wetlands, but the influence of other community changes cannot be excluded.

Despite the need for detailed further study, our findings in globally distributed wetlands indicate that this change in isomerisation with pH represents a poorly understood yet potentially widespread taxonomic or physiological signal, with potential palaeoenvironmental or geobiological utility.

4.1.3 Distinct habitat preferences of Thaumarchaeota in wetlands are revealed by the abundance and distribution of crenarchaeol

Crenarchaeol, a structurally unique isoGDGT produced by Thaumarchaeota (Sinninghe Damsté et al., 2002; Elling et al., 2017), is only present at very low abundances in all three of our primary study sites, and in most sites in the global peat database (Table S5 and S6), suggesting that these Archaea are only minor constituents of the archaeal communities in such environments (Fig. 2m-o, and Fig. 3a). This is consistent with genomic evidence from wetlands that generally indicate a low abundance or absence of Thaumarchaeota OTUs in wetlands (Lv et al., 2014; Narrowe et al., 2017; Bai et al., 2018).

The depth profile of crenarchaeol and its isomer at all sites, but particularly Sebangau, is consistent with other reports of lipids from Thaumarchaeota in wetlands (Yang et al., 2018). Crenarchaeol is most abundant at the surface because the periodically oxygenated peat surface is most likely to harbour aerobic Thaumarchaeota (Stieglmeier et al., 2014), and its abundance decreases with depth (Fig. 3m). Furthermore, crenarchaeol is most closely associated with more circumneutral pH wetlands in our CCA analysis (Fig. 5), though not in all of them, suggesting that while pH may in part regulate the abundance of Thaumarchaeota, other factors also clearly play an important role. These observations are in line with the understanding that most

726 Thaumarchaeota are neutrophilic, aerobic ammonia-oxidisers, predominantly linked in
727 mesophilic terrestrial environments to dry, well-aerated soils of circumneutral pH rather
728 than waterlogged, anoxic and often acidic peat soil or wetland sediment (Stieglmeier et
729 al., 2014; Zheng et al., 2015). Therefore, it can be said that in general, Thaumarchaeota
730 are not important contributors to the wider cyclic-GDGT pool in most wetlands, and could
731 be used as a viable tracer for drying of ancient wetlands (Zheng et al., 2015).

732 In the following section, we concentrate on the distributions of Me-GDGTs, Me-
733 GMGTs, BDGTs and PDGTs in our three primary sites.

734

735 ## 4.2 Methylated-GDGTs (Me-GDGTs) and Me-GMGTs are widespread in wetlands

736 Me-GDGTs are higher mass homologs of regular isoGDGTs, containing up to
737 three additional methylations on the biphytanyl chain and identified in culture with up to 6
738 cyclopentane rings (Knappy et al., 2015). Similarly, Me-isoGMGTs are higher mass
739 methylated homologs of the isoGMGTs (Knappy et al., 2015), a class of monoalkyl
740 tetraethers with a covalent cross link between the biphytanyl chains. Regular isoGMGTs
741 were recently identified as being abundant in peat, especially in tropical sites (Naafs et
742 al., 2018a). They have previously been identified in cultures of several methanogenic
743 Euryarchaeota: (hyper)thermophiles *Methanothermobacter thermautotrophicus* (Knappy
744 et al., 2015; Yoshinaga et al., 2015), *Methanobacter marbugensis*, *Methanosaeta*
745 *thermophila* (Bauersachs et al., 2015), and mesophiles *Methanobrevibacter smithii* and
746 *Methanosphaera stadtmanae* (Bauersachs et al., 2015). They were also detected in the
747 core lipids of the heterotrophic Euryarchaeota *Thermococcus kodakarensis* (Meador et
748 al., 2014), and in two Crenarchaeota species: *Sulfolobus acidocaldarius* and
749 *Pyrobaculum* sp. AQ1.S2 (Knappy et al., 2015). Our identification of Me-isoGDGTs and

Me-GMGTs in all three of our wetland sites is only the second time these compounds have been identified in wetlands (Yang et al., 2018). Although they do not systematically share a depth trend across the three sites, both compound classes increase relative to isoGDGT-0 below the oxic-anoxic acrotelm-catotelm boundary in Sebangau and are relatively stable with depth throughout the completely anoxic Everglades sediment profile (Fig. 2g-l). Whilst there is a putative biosynthetic link between the Me-GDGT and isoGMGT chain adaptations (Knappy, 2010; Knappy et al., 2014), 2Me-GDGTs and Me-GMGTs show different behaviour than Me-GDGTs in PCA (Fig. 3B), suggesting potentially different controls on their production. However, their depth trends in our wetland sediments, which harbour large and diverse communities of anaerobic Euryarchaeota (Cadillo-Quiroz et al., 2008; Pazinato et al., 2010; Bräuer et al., 2011; Narrowe et al., 2017), is broadly consistent with culture evidence that supports a predominant source amongst the Euryarchaeota, possibly predominantly methanogens (Knappy et al., 2015) inhabiting anaerobic niches in wetlands. This is further supported by their absence above detection limits in an oxygenated mineral soil (Yang et al., 2018), and their relatively high abundance in thermogenic compost soils, eutrophic lake sediments and Messinian marls (Knappy et al., 2014). Me-GDGTs have additionally been detected in anoxic estuarine sediments (Zhu et al., 2014), deep sub-surface marine sediments from the Peru Margin (Zhu et al., 2014), and marine hydrothermal vent sediments (Reeves et al., 2014).

The precise controls on Me-isoGDGT production are thus far unclear. Me-isoGDGT-0 production was shown to increase relative to isoGDGT-0 when detergents were added to *M. marbugensis* cultures (Grather et al., 2007), and when M. thermautotrophicus was grown outside of its normal growth temperature (at 45 °C rather

than 70 °C; Knappy et al., 2015). These findings collectively suggest that additional isoprenoid chain methylation could be a stress-response mechanism in certain Archaea. Whilst the effect of additional methylation on the isoGDGT membrane structure is not well understood, it has been suggested that chain methylation would cause a twisting of the isoGDGT backbone, modifying membrane packing tightness in a similar fashion to the addition of methyl groups at lower temperatures and higher alkalinities in brGDGT producing Bacteria (Knappy et al., 2015). We do not see evidence for this relationship in our wetland sites: the highest proportion of Me-GDGTs relative to isoGDGT-0 occurs in Sebangau, our most acidic and highest temperature site. Thus, this could be a taxonomic rather than physiological signal, linked perhaps to the putative enrichment of thermo- and/or acidophilic Archaea at this site. However, as observed with the isoGDGTs, it is possible that the level of cyclisation of Me-GDGTs also responds to temperature and pH. Their relative distribution in our sites does indeed suggest a possible environmental response in line with archaeal membrane regulation or changes in source community, with no cyclic homologs present in our circumneutral Everglades site, and the highest relative abundance of cylic Me-GDGTs ring index in Sebangau, our highest temperature and most acidic site (Table S2). More work is required to confirm this possible temperature-pH dependence.

4.3 BDGT and PDGT producers are anaerobes with a possible habitat preference for circumneutral pH wetlands

BDGTs and PDGTs are isoprenoid-based archaeal lipids that were first identified as orphan lipids in estuarine and subseafloor sediments (Zhu et al., 2014). Both sets of compounds were subsequently identified in a culture of the only isolate of the newly

identified seventh order of methanogens, *Methanomassiliicoccus luminyensis*. Screening of 25 other cultured Archaea, including members of the Euryarchaeota, Crenarchaeota and Thaumarchaeota, failed to detect BDGTs or PDGTs, suggesting that these compounds could indeed be specific biomarkers for the Methanomassiliicoccales (Becker et al., 2016). This could be a potentially unique trait alongside their distinctive H_2 dependent methylotrophic metabolism and energy conservation mechanisms (Becker et al., 2016; Kröninger et al., 2016; Kallistova et al., 2017). However, the BDGTs have also been linked to the uncultured Bathyarchaeota in estuarine sediments, based on the depth correlation of IPL-BDGTs and the Bathyarchaeota 16s gene (Meador et al., 2015). Moreover, more recent $\delta_{13}C$ characterisation of BDGTs suggested that they might have multiple archaeal sources in marine environments (Coffinet et al., 2020). This could include a mixture of autotrophic, potentially methanogenic, and heterotrophic Archaea (Coffinet et al., 2020).

Our work is the first identification of PDGTs in wetlands and only the second of BDGTs, which were recently characterised in peat from Southern China (Yang et al., 2018). As is observed for the BDGTs in the Southern Chinese peat, in our peat cores both compound classes become more abundant at depth, being absent or only present in negligible amounts within the partially oxygenated acrotelms of Sebangau and Tor Royal (Fig. 2a-f). This suggests that both BDGTs and PDGTs have a predominantly anaerobic source in wetland environments. Both BDGTs and PDGTs are significantly less abundant in acidic peatlands, and have the highest relative abundance in the Everglades, the most minerotrophic, circumneutral pH site, with intermediate relative abundances found in Tor Royal. This suggests that BDGT and PDGT producers are selected for in more neutral pH environments. Consistent with these results, the optimum growth of the

only cultured isolate of the seventh order of methanogens that produces BDGTs and PDGTs, *Methanomassiliicoccus luminyensis,* is at pH 7. In addition, *Methanomassiliicoccus* were recently identified as important members of the methanogen community in the Florida Everglades (Bae et al., 2015) as well as other wetland types (Söllinger et al., 2016), but particularly in minerotrophic wetland soils (Yang et al., 2017). This is consistent with an important input into the BDGT pool from members of the *Methanomassiliicoccus* in our Everglades site. Interestingly, the higher relative abundance of BDGTs in the IPL-derived fraction than in the core lipid fraction is mirrored by the findings of Coffinet et al., (2020), which the authors explain could be due to their preferential preservation as a result of the steric hindrance of the glycosidic bond by the additional methyl group, limiting the action of extra-cellular enzymes. This could lead to longer term preservation of IPL-BDGTs in sediments relative to other archaeal IPL types.

Whilst further work is required to validate the potential of BDGTs and PDGTs as markers for *Methanomassiliicoccus* in wetlands, our results are consistent with substantial input from this order. If confirmed, this finding would add to the growing body of evidence that suggests *Methanomassiliicoccus* play a key but previously overlooked role in the global carbon cycle, particularly in minerotrophic wetlands. It also suggests that PDGTs and BDGTs could be useful to trace the contribution of this order to wetland biogeochemistry.

5 Conclusions

We determined the relative abundances of diverse archaeal lipid types in three wetland study sites, and further contextualised these, where possible, with a re-analysis of a global database of archaeal lipids in wetlands. The latter broadly confirms that findings based

on our three in-depth study sites are representative but further global analysis is necessary. We demonstrate using multivariate methods that the degree of archaeal isoGDGT cyclisation does in fact vary in response to temperature and acidity in wetlands, consistent with archaeal membrane homeostasis. This contrasts with findings that focus on the 2-dimensional relationships of common indices such as TEX86 or Ring Index with pH or temperature in global wetlands. Intriguingly, we find that the ratio of isoGDGT isomers ($IsoGDGT_{Isomer\ Index}$) is globally correlated to pH, likely signalling a distinct, widespread and poorly understood adaptation or taxonomic signal which demands further investigation. Crenarchaeol, indicative of Thaumarchaeota, is only present in small proportions in almost all wetlands, and is more closely linked with mesophilic, minerotrophic sites. We also focus on four main newly identified archaeal core lipid groups present in our three principal wetland study sites, the Me-GDGTs, Me-GMGTs, BDGTs and PDGTs, which we identify as being abundant in wetlands. In most cases these compounds become more abundant at depth which suggests that they are produced predominantly by anaerobes. Furthermore, the BDGTs and PDGTs have depth profiles and appear to be more abundant in circumneutral wetlands, consistent with their putative source, the *Methanomassiliicoccales*, highlighting the potentially key role of this newly identified seventh order of methanogens in global carbon cycling. These findings provide a critical context for lipid-based investigations of Archaea in modern wetland environments, as well as in reconstructions of archaeal biogeochemistry and their environmental/climatic context in ancient wetland sediments.

Acknowledgments

We gratefully acknowledge T. Meador and an anonymous reviewer for their valuable comments and time on a previous version of this paper, which greatly improved this manuscript. We also thank Xavier Comas at the Department of Geosciences, Florida Atlantic University, for his hospitality and assistance in accessing and sampling in the Florida Everglades, and Mari Könönen for samples from Sebangau. J. Blewett thanks G. Inglis for useful discussions. J. Blewett is supported by a NERC GW4+ Doctoral Training Partnership studentship from the Natural Environment Research Council (NE/ L002434/1) and is thankful for the support and additional funding from CASE partner, Elementar UK Ltd. B.D.A. Naafs acknowledges funding through a Royal Society Tata University Research Fellowship. R. D. Pancost acknowledges the Advanced ERC Project "the greenhouse earth system" (T-GRES; project reference 340923). We also thank the NERC Life Sciences Mass Spectrometry Facility (Bristol) for analytical support and D. Atkinson for help with the sample preparation. Members of the T-GRES Peat Database collaborators are M.J. Amesbury, H. Biester, R. Bindler, J. Blewett, M.A. Burrows, D. del Castillo Torres, F.M. Chambers, A.D. Cohen, S.J. Feakins, M. Gałka, A. Gallego-Sala, L. Gandois, D.M. Gray, P.G. Hatcher, E.N. Honorio Coronado, P.D.M. Hughes, A. Huguet, M. Könönen, F. Laggoun-Défarge, O. Lähteenoja, M. Lamentowicz, R. Marchant, X. Pontevedra- Pombal, C. Ponton, A. Pourmand, A.M. Rizzuti, L. Rochefort, J. Schellekens, F. De Vleeschouwer.

Competing Interests

The authors declare that they have no competing interests.

References

893 Abtew, W., Obeysekera, J., Iricanin, N., 2011. Pan evaporation and potential
894 evapotranspiration trends in South Florida. Hydrological Processes 25, 958–969.
895 Amesbury, M.J., Charman, D.J., Fyfe, R.M., Langdon, P.G., West, S., 2008. Bronze
896 Age upland settlement decline in southwest England: testing the climate change
897 hypothesis. Journal of Archaeological Science 35, 87–98.
898 Andersen, R., Chapman, S.J., Artz, R.R.E., 2013. Microbial communities in natural and
899 disturbed peatlands: A review. Soil Biology and Biochemistry 57, 979–994.
900 Bae, H., Holmes, M.E., Chanton, J.P., Reddy, K.R., 2015. Distribution, Activities, and
901 Interactions of Methanogens and Sulfate- Reducing Prokaryotes in the Florida
902 Everglades. Applied and Environmental Microbiology 81, 7431–7442.
903 Bai, Y., Wang, J., Zhan, Z., Guan, L., Jin, L., Zheng, G., Huang, Z., 2018. The Variation
904 of Microbial Communities in a Depth Profile of Peat in the Gahai Lake Wetland
905 Natural Conservation Area. Geomicrobiology Journal 35, 484–490.
906 Bale, N.J., Palatinszky, M., Rijpstra, W.I.C., Herbold, C.W., Wagner, M., Damsté, J.S.S.,
907 2019. Membrane lipid composition of the moderately thermophilic ammonia-
908 oxidizing archaeon "Candidatus Nitrosotenuis uzonensis" at different growth
909 temperatures. Applied and Environmental Microbiology 85.
910 doi:10.1128/AEM.01332-19
911 Barber, K.E., 1993. Peatlands as scientific archives of past biodiversity. Biodiversity and
912 Conservation 2, 474–489.
913 Bauersachs, T., Speelman, E.N., Hopmans, E.C., Reichart, G.-J., Schouten, S.,
914 Damste, J.S.S., 2010. Fossilized glycolipids reveal past oceanic N2 fixation by
915 heterocystous cyanobacteria. Proceedings of the National Academy of Sciences
916 107, 19190–19194.

Bauersachs, T., Weidenbach, K., Schmitz, R.A., Schwark, L., 2015. Distribution of glycerol ether lipids in halophilic, methanogenic and hyperthermophilic archaea. Organic Geochemistry 83–84, 101–108.

Becker, K.W., Elling, F.J., Yoshinaga, M.Y., Söllinger, A., Urich, T., Hinrichs, K.U., 2016. Unusual butane- and pentanetriol-based tetraether lipids in Methanomassiliicoccus Luminyensis, a representative of the seventh order of methanogens. Applied and Environmental Microbiology 82, 4505–4516.

Becker, K.W., Lipp, J.S., Zhu, C., Liu, X., Hinrichs, K., 2013. An improved method for the analysis of archaeal and bacterial ether core lipids. Organic Geochemistry 61, 34–44.

Besseling, M.A., Hopmans, E.C., Christine Boschman, R., Sinninghe Damsté, J.S., Villanueva, L., 2018. Benthic archaea as potential sources of tetraether membrane lipids in sediments across an oxygen minimum zone. Biogeosciences 15, 4047–4064.

Bligh, E., Dyer, W., 1959. A Rapid Method of Total Lipid Extraction and Purification. Canadian Journal of Biochemistry and Physiology 37.

Borcard, D., Gillet, F., Legendre, P., 2018. Numerical Ecology with R. Springer International.

Boyd, E.S., Pearson, A., Pi, Y., Li, W.J., Zhang, Y.G., He, L., Zhang, C.L., Geesey, G.G., 2011. Temperature and pH controls on glycerol dibiphytanyl glycerol tetraether lipid composition in the hyperthermophilic crenarchaeon Acidilobus sulfurireducens. Extremophiles 15, 59–65.

Braak, C.J.F.F., Verdonschot, P.F.M.M., 1995. Canonical correspondence analysis and related multivariate methods in aquatic ecology. Aquatic Sciences 57, 255–289.

941 Bräuer, S.L., Cadillo-Quiroz, H., Ward, R.J., Yavitt, J.B., Zinder, S.H., 2011.
942 Methanoregula boonei gen. nov., sp. nov., an acidiphilic methanogen isolated from
943 an acidic peat bog. International Journal of Systematic and Evolutionary
944 Microbiology 61, 45–52.
945 Bridgham, S.D., Cadillo-Quiroz, H., Keller, J.K., Zhuang, Q., 2013. Methane emissions
946 from wetlands: Biogeochemical, microbial, and modeling perspectives from local to
947 global scales. Global Change Biology 19, 1325–1346.
948 Buckles, L.K., Villanueva, L., Weijers, J.W.H., Verschuren, D., Damsté, J.S.S., 2013.
949 Linking isoprenoidal GDGT membrane lipid distributions with gene abundances of
950 ammonia-oxidizing Thaumarchaeota and uncultured crenarchaeotal groups in the
951 water column of a tropical lake (Lake Challa, East Africa). Environmental
952 Microbiology 15, 2445–2462.
953 Burt, T.P., Holden, J., 2010. Changing temperature and rainfall gradients in the British
954 Uplands. Climate Research 45, 57–70.
955 Cadillo-Quiroz, H., Bräuer, S., Yashiro, E., Sun, C., Yavitt, J., Zinder, S., 2006. Vertical
956 profiles of methanogenesis and methanogens in two contrasting acidic peatlands in
957 central New York State, USA. Environmental Microbiology 8, 1428–1440.
958 Cadillo-Quiroz, H., Yashiro, E., Yavitt, J.B., Zinder, S.H., 2008. Characterization of the
959 archaeal community in a minerotrophic fen and terminal restriction fragment length
960 polymorphism-directed isolation of a novel hydrogenotrophic methanogen. Applied
961 and Environmental Microbiology 74, 2059–2068.
962 Caforio, A., Driessen, A.J.M., 2017. Archaeal phospholipids: Structural properties and
963 biosynthesis. Biochimica et Biophysica Acta - Molecular and Cell Biology of Lipids
964 1862, 1325–1339.

965 Castro, H., Ogram, A., Reddy, K.R., 2004. Phylogenetic characterization of
966 methanogenic assemblages in eutrophic and oligotrophic areas of the Florida
967 everglades. Applied and Environmental Microbiology 70, 6559–6568.
968 Charman, D.J., Aravena, R., Bryant, C.L., Harkness, D.D., 1999. Carbon isotopes in
969 peat, DOC, CO2, and CH4 in a holocene peatland on Dartmoor, southwest
970 England. Geology 27, 539–542.
971 Chaves-Torres, L., Pancost, R.D., 2016. Insoluble prokaryotic membrane lipids in a
972 Sphagnum peat: Implications for organic matter preservation. Organic
973 Geochemistry 93, 77–91.
974 Chong, P.L.G., Ayesa, U., Prakash Daswani, V., Hur, E.C., 2012. On physical
975 properties of tetraether lipid membranes: Effects of cyclopentane rings. Archaea
976 2012. doi:10.1155/2012/138439
977 Chong, P.L.G., Ravindra, R., Khurana, M., English, V., Winter, R., 2005. Pressure
978 perturbation and differential scanning calorimetric studies of bipolar tetraether
979 liposomes derived from the thermoacidophilic archaeon Sulfolobus acidocaldarius.
980 Biophysical Journal 89, 1841–1849.
981 Chugunov, A.O., Volynsky, P.E., Krylov, N.A., Boldyrev, I.A., Efremov, R.G., 2014.
982 Liquid but durable: Molecular dynamics simulations explain the unique properties of
983 archaeal-like membranes. Scientific Reports 4, 1–8.
984 Coffinet, S., Huguet, A., Bergonzini, L., Pedentchouk, N., Williamson, D., Anquetil, C.,
985 Gałka, M., Kołaczek, P., Karpińska-Kołaczek, M., Majule, A., Laggoun-Défarge, F.,
986 Wagner, T., Derenne, S., 2018. Impact of climate change on the ecology of the
987 Kyambangunguru crater marsh in southwestern Tanzania during the Late
988 Holocene. Quaternary Science Reviews 196, 100–117.

989 Coffinet, S., Huguet, A., Williamson, D., Bergonzini, L., Anquetil, C., Majule, A.,
990 Derenne, S., 2015. Occurrence and distribution of glycerol dialkanol diethers and
991 glycerol dialkyl glycerol tetraethers in a peat core from SW Tanzania. Organic
992 Geochemistry 83–84, 170–177.
993 Coffinet, S., Meador, T.B., Mühlena, L., Becker, K.W., Schröder, J., Zhu, Q.Z., Lipp,
994 J.S., Heuer, V.B., Crump, M.P., Hinrichs, K.U., 2020. Structural elucidation and
995 environmental distributions of butanetriol and pentanetriol dialkyl glycerol
996 tetraethers (BDGTs and PDGTs). Biogeosciences 17, 317–330.
997 Collins, M., Knutti, R., Arblaster, J., Dufresne, J.-L., T. Fichefet, P., Friedlingstein, X.,
998 Gao, W.J., Gutowski, T., Johns, G. Krinner, M., Shongwe, C., A.J, T., Wehner, W.
999 and M., 2013. Long-term Climate Change: Projections, Commitments and
1000 Irreversibility. Climate Change 2013: The Physical Science Basis. Contribution of
1001 Working Group I to the Fifth Assessment Report of the Intergovernmental Panel on
1002 Climate Change 1029–1136.
1003 Damsté, J.S.S., Schouten, S., Hopmans, E.C., van Duin, A.C.T., Geenevasen, J.A.J.,
1004 2002. Crenarchaeol: the characteristic core glycerol dibiphytanyl glycerol
1005 tetraether membrane lipid of cosmopolitan pelagic crenarchaeota. Journal of Lipid
1006 Research 43, 1641–1651.
1007 Dannenmuller, O., Arakawa, K., Eguchi, T., Kakinuma, K., Blanc, S., Albrecht, A.-M.,
1008 Schmutz, M., Nakatani, Y., Ourisson, G., 2000. Membrane Properties of Archæal
1009 Macrocyclic Diether Phospholipids. Chemistry - A European Journal 6, 645–654.
1010 De Rosa, M., Esposito, E., Gambacorta, A., Nicolaus, B., Bu'Lock, J.D., 1980. Effects of
1011 temperature on ether lipid composition of Caldariella acidophila. Phytochemistry
1012 19, 827–831.

De Rosa, M., Gambacorta, A., 1988. The Lipids of Archaebacteria. Progress in Lipid Research 27, 153–175.

de Rosa, M., Gambacorta, A., Gliozzi, A., 1986. Structure, Biosynthesis, and Physicochemical Properties of Archaebacterial Lipids. Microbiological Reviews 50, 70–80.

De Rosa, M., Morana, A., Riccio, A., Gambacorta, A., Trincone, A., Incani, O., 1994. Lipids of the Archaea: a new tool for bioelectronics. Biosensors and Bioelectronics 669–675.

Dean, J.F., Middelburg, J.J., Röckmann, T., Aerts, R., Blauw, L.G., Egger, M., Jetten, M.S.M., de Jong, A.E.E., Meisel, O.H., Rasigraf, O., Slomp, C.P., in't Zandt, M.H., Dolman, A.J., 2018. Methane Feedbacks to the Global Climate System in a Warmer World. Reviews of Geophysics 56, 207–250.

Delgado-Baquerizo, M., Oliverio, A.M., Brewer, T.E., Benavent-González, A., Eldridge, D.J., Bardgett, R.D., Maestre, F.T., Singh, B.K., Fierer, N., 2018. A global atlas of the dominant bacteria found in soil. Science 359, 320–325.

Elling, F.J., Könneke, M., Lipp, J.S., Becker, K.W., Gagen, E.J., Hinrichs, K.-U., 2014. Effects of growth phase on the membrane lipid composition of the thaumarchaeon *Nitrosopumilus maritimus* and their implications for archaeal lipid distributions in the marine environment. Geochimica et Cosmochimica Acta 141, 579–597.

Elling, F.J., Könneke, M., Mußmann, M., Greve, A., Hinrichs, K.U., 2015. Influence of temperature, pH, and salinity on membrane lipid composition and TEX86of marine planktonic thaumarchaeal isolates. Geochimica et Cosmochimica Acta 171, 238–255.

Elling, F.J., Könneke, M., Nicol, G.W., Stieglmeier, M., Bayer, B., Spieck, E., de la Torre,

J.R., Becker, K.W., Thomm, M., Prosser, J.I., Herndl, G.J., Schleper, C., Hinrichs, K.U., 2017. Chemotaxonomic characterisation of the thaumarchaeal lipidome. Environmental Microbiology 19, 2681–2700.

Evans, T.W., Könneke, M., Lipp, J.S., Adhikari, R.R., Taubner, H., Elvert, M., Hinrichs, K.U., 2018. Lipid biosynthesis of Nitrosopumilus maritimus dissected by lipid specific radioisotope probing (lipid-RIP) under contrasting ammonium supply. Geochimica et Cosmochimica Acta 242, 51–63.

Gabriel, J.L., Lee Gau Chong, P., 2000. Molecular modeling of archaebacterial bipolar tetraether lipid membranes. Chemistry and Physics of Lipids 105, 193–200.

Gallego-Sala, A. V., Colin Prentice, I., 2013. Blanket peat biome endangered by climate change. Nature Climate Change 3, 152–155.

Gong, L., Wang, H., Xiang, X., Qiu, X., Liu, Q., Wang, R., Zhao, R., Wang, C., 2015. pH Shaping the Composition of sqhC-Containing Bacterial Communities. Geomicrobiology Journal 32, 433–444.

Grather, O., Arigoni, D., 1995. Regioisomeric Macrocyclic Tetraethers in the Lipids of. J. Chem. Soc. Chem. Commun 0, 405–406.

Grather, O., Arigoni, D., Fitz, W., Riimmler, M., Galliker, P., 2007. New Structural and Biosynthetic Aspects of the Unusual Core Lipids from Archaebacteria, in: Vitamin B 12 and B 12 -Proteins . doi:10.1002/9783527612192.ch29

Harvey, R., Fallon, R., Patton, J., 1986. The effect of organic matter and oxygen on the degradation of bacterial membrane lipids in marine sediments. Geochimica et Cosmochimica Acta 50, 795–804.

Hopmans, E.C., Schouten, S., Sinninghe Damsté, J.S., 2016. The effect of improved chromatography on GDGT-based palaeoproxies. Organic Geochemistry 93, 1–6.

Huguet, A., Fosse, C., Laggoun-Défarge, F., Toussaint, M.L., Derenne, S., 2010. Occurrence and distribution of glycerol dialkyl glycerol tetraethers in a French peat bog. Organic Geochemistry 41, 559–572.

Huguet, C., Fietz, S., Rosell-Melé, A., Daura, X., Costenaro, L., 2017. Molecular dynamics simulation study of the effect of glycerol dialkyl glycerol tetraether hydroxylation on membrane thermostability. Biochimica et Biophysica Acta - Biomembranes 1859, 966–974.

Hurley, S.J., Elling, F.J., Könneke, M., Buchwald, C., Wankel, S.D., Santoro, A.E., Lipp, J.S., Hinrichs, K.U., Pearson, A., 2016. Influence of ammonia oxidation rate on thaumarchaeal lipid composition and the TEX86 temperature proxy. Proceedings of the National Academy of Sciences of the United States of America 113, 7762–7767.

Inglis, G.N., Farnsworth, A., Collinson, M.E., Carmichael, M.J., Naafs, B.D.A., Lunt, D.J., Valdes, P.J., Pancost, R.D., 2019. Terrestrial environmental change across the onset of the PETM and the associated impact on biomarker proxies: A cautionary tale. Global and Planetary Change 181, 102991.

Jackson, C.R., Liew, K.C., Yule, C.M., 2009. Structural and functional changes with depth in microbial communities in a tropical malaysian peat swamp forest. Microbial Ecology 57, 402–412.

Jiang, Y.J., He, W., Liu, W.X., Qin, N., Ouyang, H.L., Wang, Q.M., Kong, X.Z., He, Q.S., Yang, C., Yang, B., Xu, F.L., 2014. The seasonal and spatial variations of phytoplankton community and their correlation with environmental factors in a large eutrophic Chinese lake (Lake Chaohu). Ecological Indicators 40, 58–67.

Kallistova, A.Y., Merkel, A.Y., Tarnovetskii, I.Y., Pimenov, N. V., 2017. Methane

formation and oxidation by prokaryotes. Microbiology 86, 671–691.

Kaplan, J.O., Bigelow, N.H., Prentice, I.C., Harrison, S.P., Bartlein, P.J., Christensen, T.R., Cramer, W., Matveyeva, N. V., McGuire, A.D., Murray, D.F., Razzhivin, V.Y., Smith, B., Walker, D.A., Anderson, P.M., Andreev, A.A., Brubaker, L.B., Edwards, M.E., Lozhkin, A. V., 2003. Climate change and Arctic ecosystems: 2. Modeling, paleodata-model comparisons, and future projections. Journal of Geophysical Research D: Atmospheres 108. doi:10.1029/2002jd002559

King, G.M., Roslev, P., Skovgaard, H., 1990. Distribution and rate of methane oxidation in sediments of the Florida Everglades. Applied and Environmental Microbiology 56, 2902–2911.

Knappy, C., Barillà, D., Chong, J., Hodgson, D., Morgan, H., Suleman, M., Tan, C., Yao, P., Keely, B., 2015. Mono-, di- and trimethylated homologues of isoprenoid tetraether lipid cores in archaea and environmental samples: Mass spectrometric identification and significance. Journal of Mass Spectrometry 50, 1420–1432.

Knappy, C.S., 2010. Mass spectrometric studies of ether lipids in Archaea and sediments. Ph.D. Thesis.

Knappy, C.S., Barill, D., De Blaquiere, J.P.A., Morgan, H.W., Nunn, C.E.M., Suleman, M., Tan, C.H.W., Keely, B.J., 2012. Structural complexity in isoprenoid glycerol dialkyl glycerol tetraether lipid cores of Sulfolobus and other archaea revealed by liquid chromatography-tandem mass spectrometry. Chemistry and Physics of Lipids 165, 648–655.

Knappy, C.S., Yao, P., Pickering, M.D., Keely, B.J., 2014. Identification of homoglycerol- and dihomoglycerol-containing isoprenoid tetraether lipid cores in aquatic sediments and a soil. Organic Geochemistry 76, 146–156.

1109 Könönen, M., Jauhiainen, J., Laiho, R., Kusin, K., Vasander, H., 2015. Physical and
1110 chemical properties of tropical peat under stabilised land uses. Mires and Peat 16,
1111 1–13.
1112 Könönen, M., Jauhiainen, J., Laiho, R., Spetz, P., Kusin, K., Limin, S., Vasander, H.,
1113 2016. Land use increases the recalcitrance of tropical peat. Wetlands Ecology and
1114 Management 24, 717–731.
1115 Kröninger, L., Berger, S., Welte, C., Deppenmeier, U., 2016. Evidence for the
1116 involvement of two heterodisulfide reductases in the energy-conserving system of
1117 Methanomassiliicoccus luminyensis. FEBS Journal 283, 472–483.
1118 Lengger, S.K., Kraaij, M., Tjallingii, R., Baas, M., Stuut, J.B., Hopmans, E.C., Sinninghe
1119 Damsté, J.S., Schouten, S., 2013. Differential degradation of intact polar and core
1120 glycerol dialkyl glycerol tetraether lipids upon post-depositional oxidation. Organic
1121 Geochemistry 65, 83–93.
1122 Lengger, S.K., Lipsewers, Y.A., De Haas, H., Sinninghe Damsté, J.S., Schouten, S.,
1123 2014. Lack of 13 C-label incorporation suggests low turnover rates of
1124 thaumarchaeal intact polar tetraether lipids in sediments from the Iceland shelf.
1125 Biogeosciences 11, 201–216.
1126 Lipp, J.S., Hinrichs, K.U., 2009. Structural diversity and fate of intact polar lipids in
1127 marine sediments. Geochimica et Cosmochimica Acta 73, 6816–6833.
1128 Lipp, J.S., Morono, Y., Inagaki, F., Hinrichs, K.U., 2008. Significant contribution of
1129 Archaea to extant biomass in marine subsurface sediments. Nature 454, 991–994.
1130 Liu, X.L., De Santiago Torio, A., Bosak, T., Summons, R.E., 2016. Novel archaeal
1131 tetraether lipids with a cyclohexyl ring identified in Fayetteville Green Lake, NY, and
1132 other sulfidic lacustrine settings. Rapid Communications in Mass Spectrometry 30,

1133 1197–1205.

1134 Liu, X.L., Lipp, J.S., Birgel, D., Summons, R.E., Hinrichs, K.U., 2018. Predominance of
1135 parallel glycerol arrangement in archaeal tetraethers from marine sediments:
1136 Structural features revealed from degradation products. Organic Geochemistry
1137 115, 12–23.

1138 Liu, X.L., Russell, D.A., Bonfio, C., Summons, R.E., 2019. Glycerol configurations of
1139 environmental GDGTs investigated using a selective sn2 ether cleavage protocol.
1140 Organic Geochemistry 128, 57–62.

1141 Liu, X.L., Summons, R.E., Hinrichs, K.U., 2012. Extending the known range of glycerol
1142 ether lipids in the environment: Structural assignments based on tandem mass
1143 spectral fragmentation patterns. Rapid Communications in Mass Spectrometry 26,
1144 2295–2302.

1145 Logemann, J., Graue, J., Köster, J., Engelen, B., Rullkötter, J., Cypionka, H., 2011. A
1146 laboratory experiment of intact polar lipid degradation in sandy sediments.
1147 Biogeosciences 8, 2547–2560.

1148 Lv, X., Yu, J., Fu, Y., Ma, B., Qu, F., Ning, K., Wu, H., 2014. A meta-analysis of the
1149 bacterial and archaeal diversity observed in wetland soils. Scientific World Journal
1150 2014. doi:10.1155/2014/437684

1151 Meador, T.B., Bowles, M., Lazar, C.S., Zhu, C., Teske, A., Hinrichs, K.U., 2015. The
1152 archaeal lipidome in estuarine sediment dominated by members of the
1153 Miscellaneous Crenarchaeotal Group. Environmental Microbiology 17, 2441–2458.

1154 Meador, T.B., Gagen, E.J., Loscar, M.E., Goldhammer, T., Yoshinaga, M.Y., Wendt, J.,
1155 Thomm, M., Hinrichs, K.U., 2014. Thermococcus kodakarensis modulates its polar
1156 membrane lipids and elemental composition according to growth stage and

1157 phosphate availability. Frontiers in Microbiology 5, 1–13.
1158 Naafs, B.D.A., Inglis, G.N., Blewett, J., McClymont, E.L., Lauretano, V., Xie, S.,
1159 Evershed, R.P., Pancost, R.D., 2019. The potential of biomarker proxies to trace
1160 climate, vegetation, and biogeochemical processes in peat: A review. Global and
1161 Planetary Change 179, 57–79.
1162 Naafs, B.D.A., Inglis, G.N., Zheng, Y., Amesbury, M.J., Biester, H., Bindler, R., Blewett,
1163 J., Burrows, M.A., del Castillo Torres, D., Chambers, F.M., Cohen, A.D., Evershed,
1164 R.P., Feakins, S.J., Gałka, M., Gallego-Sala, A., Gandois, L., Gray, D.M., Hatcher,
1165 P.G., Honorio Coronado, E.N., Hughes, P.D.M., Huguet, A., Könönen, M.,
1166 Laggoun-Défarge, F., Lähteenoja, O., Lamentowicz, M., Marchant, R., McClymont,
1167 E., Pontevedra-Pombal, X., Ponton, C., Pourmand, A., Rizzuti, A.M., Rochefort, L.,
1168 Schellekens, J., De Vleeschouwer, F., Pancost, R.D., 2017. Introducing global
1169 peat-specific temperature and pH calibrations based on brGDGT bacterial lipids.
1170 Geochimica et Cosmochimica Acta 208, 285–301.
1171 Naafs, B.D.A., McCormick, D., Inglis, G.N., Pancost, R.D., 2018a. Archaeal and
1172 bacterial H-GDGTs are abundant in peat and their relative abundance is positively
1173 correlated with temperature. Geochimica et Cosmochimica Acta 227, 156–170.
1174 Naafs, B.D.A., Rohrssen, M., Inglis, G.N., Lähteenoja, O., Feakins, S.J., Collinson, M.E.,
1175 Kennedy, E.M., Singh, P.K., Singh, M.P., Lunt, D.J., Pancost, R.D., 2018b. High
1176 temperatures in the terrestrial mid-latitudes during the early Palaeogene. Nature
1177 Geoscience 11, 766–771.
1178 Narrowe, A.B., Angle, J.C., Daly, R.A., Stefanik, K.C., Wrighton, K.C., Miller, C.S.,
1179 2017. High-resolution sequencing reveals unexplored archaeal diversity in
1180 freshwater wetland soils. Environmental Microbiology 19, 2192–2209.

Oksanen, J., Kindt, R., Legendre, P., O'Hara, B., Simpson, G.L., Solymos, P.M., Stevens, M.H.H., & Wagner, H., 2017. Vegan: Community ecology package [WWW Document]. Community ecology package. URL https://cran.r-project.org/web/packages/vegan/index.html

Page, S.E., Rieley, J.O., Shotyk, O.W., Weiss, D., 1999. Interdependence of peat and vegetation in a tropical peat swamp forest. Philosophical Transactions of the Royal Society B: Biological Sciences 354, 1885–1897.

Page, S.E., Wust, R.A.J., Weiss, D., Rieley, J.O., Shotyk, W., Limin, S.H., 2004. A record of Late Pleistocene and Holocene carbon accumulation and climate change from an equatorial peat bog (Kalimantan, Indonesia): Implications for past, present and future carbon dynamics. Journal of Quaternary Science 19, 625–635.

Pancost, R.D., Baas, M., Van, B., Sinninghe, J.S., Van Geel, B., Sinninghe Damsté, J.S., 2003. Response of an ombrotrophic bog to a regional climate event revealed by macrofossil, molecular and carbon isotopic data. Holocene 13, 921–932.

Pancost, R.D., Sinninghe Damsté, J.S., 2003. Carbon isotopic compositions of prokaryotic lipids as tracers of carbon cycling in diverse settings. Chemical Geology 195, 29–58.

Pancost, R.D., Steart, D.S., Handley, L., Collinson, M.E., Hooker, J.J., Scott, A.C., Grassineau, N. V., Glasspool, I.J., 2007. Increased terrestrial methane cycling at the Palaeocene-Eocene thermal maximum. Nature 449, 332–335.

Pazinato, J.M., Paulo, E.N., Mendes, L.W., Vazoller, R.F., Tsai, S.M., 2010. Molecular characterization of the archaeal community in an Amazonian wetland soil and culture-dependent isolation of methanogenic archaea. Diversity 2, 1026–1047.

Pearson, A., Huang, Z., Ingalls, A.E., Romanek, C.S., Wiegel, J., Freeman, K.H.,

Smittenberg, R.H., Zhang, C.L., 2004. Nonmarine crenarchaeol in Nevada hot springs. Applied and Environmental Microbiology 70, 5229–5237.

Pearson, A., Pi, Y., Zhao, W., Li, W.J., Li, Y., Inskeep, W., Perevalova, A., Romanek, C., Li, S., Zhang, C.L., 2008. Factors controlling the distribution of archaeal tetraethers in terrestrial hot springs. Applied and Environmental Microbiology 74, 3523–3532.

Pester, M., Schleper, C., Wagner, M., 2011. The Thaumarchaeota: An emerging view of their phylogeny and ecophysiology. Current Opinion in Microbiology 14, 300–306.

Peterse, F., Hopmans, E.C., Schouten, S., Mets, A., Rijpstra, W.I.C., Sinninghe Damsté, J.S., 2011. Identification and distribution of intact polar branched tetraether lipids in peat and soil. Organic Geochemistry 42, 1007–1015.

Pitcher, A., Schouten, S., Sinninghe Damsté, J.S., 2009. In situ production of crenarchaeol in two California hot springs. Applied and Environmental Microbiology 75, 4443–4451.

Qin, W., Carlson, L.T., Armbrust, E.V., Devol, A.H., Moffett, J.W., Stahl, D.A., Ingalls, A.E., 2015. Confounding effects of oxygen and temperature on the TEX 86 signature of marine Thaumarchaeota. Proceedings of the National Academy of Sciences of the United States of America 112, 10979–10984.

Reeves, E.P., Yoshinaga, M.Y., Pjevac, P., Goldenstein, N.I., Peplies, J., Meyerdierks, A., Amann, R., Bach, W., Hinrichs, K.U., 2014. Microbial lipids reveal carbon assimilation patterns on hydrothermal sulfide chimneys. Environmental Microbiology 16, 3515–3532.

Schouten, S., Forster, A., Panoto, E.F., Sinninghe Damsté, J.S., 2007. Towards calibration of the TEX86 palaeothermometer for tropical sea surface temperatures in ancient greenhouse worlds. Organic Geochemistry 38, 1537–1546.

1229 Schouten, S., Hopmans, E.C., Schefuß, E., Sinninghe Damsté, J.S., 2002. Distributional
1230 variations in marine crenarchaeotal membrane lipids: a new tool for reconstructing
1231 ancient sea water temperatures? Earth and Planetary Science Letters 204, 265–
1232 274.
1233 Schouten, S., Hopmans, E.C., Sinninghe Damsté, J.S., 2013. The organic geochemistry
1234 of glycerol dialkyl glycerol tetraether lipids: A review. Organic Geochemistry 54,
1235 19–61.
1236 Segarra, K.E. a., Schubotz, F., Samarkin, V., Yoshinaga, M.Y., Hinrichs, K.-U., Joye,
1237 S.B., 2015. High rates of anaerobic methane oxidation in freshwater wetlands
1238 reduce potential atmospheric methane emissions. Nature Communications 6,
1239 7477.
1240 Shinoda, W., Shinoda, K., Baba, T., Mikami, M., 2005. Molecular dynamics study of
1241 bipolar tetraether lipid membranes. Biophysical Journal 89, 3195–3202.
1242 Sinninghe Damsté, J.S., Hopmans, E.C., Pancost, R.D., Schouten, S., Geenevasen,
1243 J.A.J., 2000. Newly discovered non-isoprenoid glycerol dialkyl glycerol tetraether
1244 lipids in sediments. Chem Commun. 17, 1683–1684.
1245 Sinninghe Damsté, J.S., Ossebaar, J., Schouten, S., Verschuren, D., 2012a.
1246 Distribution of tetraether lipids in the 25-ka sedimentary record of Lake Challa:
1247 Extracting reliable TEX 86 and MBT/CBT palaeotemperatures from an equatorial
1248 African lake. Quaternary Science Reviews. doi:10.1016/j.quascirev.2012.07.001
1249 Sinninghe Damsté, J.S., Rijpstra, W.I.C., Hopmans, E.C., den Uijl, M.J., Weijers, J.W.H.,
1250 Schouten, S., 2018. The enigmatic structure of the crenarchaeol isomer. Organic
1251 Geochemistry 124, 22–28.
1252 Sinninghe Damsté, J.S., Rijpstra, W.I.C., Hopmans, E.C., Jung, M.Y., Kim, J.G., Rhee,

S.K., Stieglmeier, M., Schleper, C., 2012b. Intact polar and core glycerol dibiphytanyl glycerol tetraether lipids of group I.1a and I.1b Thaumarchaeota in soil. Applied and Environmental Microbiology 78, 6866–6874.

Söllinger, A., Schwab, C., Weinmaier, T., Loy, A., Tveit, A.T., Schleper, C., Urich, T., 2016. Phylogenetic and genomic analysis of Methanomassiliicoccales in wetlands and animal intestinal tracts reveals clade-specific habitat preferences. FEMS microbiology ecology 92, 1–12.

Stieglmeier, M., Alves, R.J.E., Schleper, C., 2014. The phylum thaumarchaeota, in: The Prokaryotes: Other Major Lineages of Bacteria and The Archaea. Springer Berlin Heidelberg, Berlin, Heidelberg, pp. 347–362.

Sundari, S., Hirano, T., Yamada, H., Kusin, K., Limin, S., 2012. Effect of groundwater level on soil respiration in tropical peat swamp forests. Journal of Agricultural Meteorology 68, 121–134.

Tian, H., Chen, G., Lu, C., Xu, X., Ren, W., Zhang, B., Banger, K., Tao, B., Pan, S., Liu, M., Zhang, C., Bruhwiler, L., Wofsy, S., 2015. Global methane and nitrous oxide emissions from terrestrial ecosystems due to multiple environmental changes. Ecosystem Health and Sustainability 1, art4.

Tripathi, B.M., Kim, M., Tateno, R., Kim, W., Wang, J., Lai-Hoe, A., Nor, N.A., Rahim, R.A., Go, R., Adams, J.M., 2015. Soil pH and biome are both key determinants of soil archaeal community structure. Soil Biology and Biochemistry 88, 1–8.

Uda, I., Sugai, A., Itoh, Y.H., Itoh, T., 2001. Variation in molecular species of polar lipids from Thermoplasma acidophilum depends on growth temperature. Lipids 36, 103–105.

Valenzuela, E.I., Prieto-Davó, A., López-Lozano, N.E., Hernández-Eligio, A., Vega-

Alvarado, L., Juárez, K., García-González, A.S., López, M.G., Cervantes, F.J., 2017. Anaerobic methane oxidation driven by microbial reduction of natural organic matter in a tropical wetland. Applied and Environmental Microbiology 83, 1–15.

Wang, H., Waldon, M.G., Meselhe, E. a, Arceneaux, J.C., Chen, C., Harwell, M.C., 2007. Surface water sulfate dynamics in the northern Florida Everglades. Journal of Environmental Quality 38, 734–41.

Wania, R., Melton, J.R., Hodson, E.L., Poulter, B., Ringeval, B., Spahni, R., Bohn, T., Avis, C.A., Chen, G., Eliseev, A. V., Hopcroft, P.O., Riley, W.J., Subin, Z.M., Tian, H., Van Bodegom, P.M., Kleinen, T., Yu, Z.C., Singarayer, J.S., Zürcher, S., Lettenmaier, D.P., Beerling, D.J., Denisov, S.N., Prigent, C., Papa, F., Kaplan, J.O., 2013. Present state of global wetland extent and wetland methane modelling: Methodology of a model inter-comparison project (WETCHIMP). Geoscientific Model Development 6, 617–641.

Weijers, J.W.H., Lim, K.L.H., Aquilina, A., Damsté, J.S.S., Pancost, R.D., 2011. Biogeochemical controls on glycerol dialkyl glycerol tetraether lipid distributions in sediments characterized by diffusive methane flux. Geochemistry, Geophysics, Geosystems 12, 1–15.

Weijers, J.W.H., Schouten, S., Van Der Linden, M., Van Geel, B., Sinninghe Damsté, J.S., 2004. Water table related variations in the abundance of intact archaeal membrane lipids in a Swedish peat bog. FEMS Microbiology Letters 239, 51–56.

White, A.D.C., Davis, W.M., Nickels, J.S., King, J.D., Bobbie, R.J., 1979. Determination of the sedimentary microbial biomass by extractable lipid phosphate. Oecologia 40, 51–62.

Wright, W., Comas, X., 2016. Estimating methane gas production in peat soils of the Florida Everglades using hydrogeophysical methods. Journal of Geophysical Research G: Biogeosciences 121, 1190–1202.

Wuchter, C., Schouten, S., Coolen, M.J.L., Sinninghe Damsté, J.S., 2004. Temperature-dependent variation in the distribution of tetraether membrane lipids of marine Crenarchaeota: Implications for TEX86 paleothermometry. Paleoceanography 19, 1–10.

Xie, S., Lipp, J.S., Wegener, G., Ferdelman, T.G., Hinrichs, K.-U., 2013. Turnover of microbial lipids in the deep biosphere and growth of benthic archaeal populations. Proceedings of the National Academy of Sciences 110, 6010–6014.

Yang, H., Pancost, R.D., Jia, C., Xie, S., 2016. The Response of Archaeal Tetraether Membrane Lipids in Surface Soils to Temperature: A Potential Paleothermometer in Paleosols. Geomicrobiology Journal 33, 98–109.

Yang, H., Xiao, W., Słowakiewicz, M., Ding, W., Ayari, A., Dang, X., Pei, H., 2018. Depth-dependent variation of archaeal ether lipids along soil and peat profiles from southern China: implications for the use of isoprenoidal GDGTs as environmental tracers. Organic Geochemistry 128, 42–56.

Yang, S., Liebner, S., Winkel, M., Alawi, M., Horn, F., Dörfer, C., Ollivier, J., He, J. sheng, Jin, H., Kühn, P., Schloter, M., Scholten, T., Wagner, D., 2017. In-depth analysis of core methanogenic communities from high elevation permafrost-affected wetlands. Soil Biology and Biochemistry 111, 66–77.

Yoshinaga, M.Y., Gagen, E.J., Wörmer, L., Broda, N.K., Meador, T.B., Wendt, J., Thomm, M., Hinrichs, K.U., 2015. Methanothermobacter thermautotrophicus modulates its membrane lipids in response to hydrogen and nutrient availability.

Frontiers in Microbiology 6, 1–9.

Zheng, Y., Li, Q., Wang, Z., Naafs, B.D.A., Yu, X., Pancost, R.D., 2015. Peatland GDGT records of Holocene climatic and biogeochemical responses to the Asian Monsoon. Organic Geochemistry 87, 86–95.

Zheng, Y., Pancost, R.D., Naafs, B.D.A., Li, Q., Liu, Z., Yang, H., 2018. Transition from a warm and dry to a cold and wet climate in NE China across the Holocene. Earth and Planetary Science Letters. doi:10.1016/j.epsl.2018.04.019

Zheng, Y., Zhou, W., Meyers, P.A., 2011. Proxy value of n-alkan-2-ones in the Hongyuan peat sequence to reconstruct Holocene climate changes on the eastern margin of the Tibetan Plateau. Chemical Geology 288, 97–104.

Zhou, A., Weber, Y., Chiu, B.K., Elling, F.J., Cobban, A.B., Pearson, A., Leavitt, W.D., 2020. Energy flux controls tetraether lipid cyclization in Sulfolobus acidocaldarius. Environmental Microbiology 22, 343–353.

Zhu, B., van Dijk, G., Fritz, C., Smolders, A.J.P., Pol, A., Jetten, M.S.M., Ettwiga, K.F., 2012. Anaerobic oxidization of methane in a minerotrophic peatland: Enrichment of nitrite-dependent methane-oxidizing bacteria. Applied and Environmental Microbiology 78, 8657–8665.

Zhu, C., Meador, T.B., Dummann, W., Hinrichs, K.U., 2014. Identification of unusual butanetriol dialkyl glycerol tetraether and pentanetriol dialkyl glycerol tetraether lipids in marine sediments. Rapid Communications in Mass Spectrometry 28, 332–338.